

Sec. 6 22 (21)
C 212NA



DEPARTMENT OF
ENERGY, MINES AND RESOURCES
MINES BRANCH
OTTAWA

*DESIGN CRITERIA FOR MULTI-WIRE
BOREHOLE EXTENSOMETER SYSTEMS*

DEPT. OF ENERGY, MINES AND RESOURCES
MINES BRANCH
SEP 25 1971
LIBRARY
OTTAWA, CANADA

D. G. F. HEDLEY

Reprinted from Proceedings of the First Canadian Symposium on Mining
Surveying and Rock Deformation Measurements, October, 1969, Fredericton,
pp. 349-377. The Canadian Institute of Surveying, Ottawa, 1970.

*UNDERGROUND MEASUREMENTS IN
A STEEPLY DIPPING OREBODY*

D. G. F. Hedley, G. Zahary, H. W. Soderlund and D. F. Coates

Reprinted from Proceedings of the 5th Canadian Rock Mechanics Symposium,
Toronto, December, 1968, pp. 105-125, Mines Branch,
Queen's Printer, Ottawa, 1969.

© Crown Copyrights reserved

Available by mail from Information Canada, Ottawa
and at the following Information Canada bookshops

HALIFAX
1735 Barrington Street

MONTREAL
Aeterna-Vie Building, 1182 St. Catherine St. West

OTTAWA
171 Slater Street

TORONTO
221 Yonge Street

WINNIPEG
Mall Center Bldg., 499 Portage Avenue

VANCOUVER
657 Granville Street

or through your bookseller

Price 25 cents Catalogue No. M38-8/103

Price subject to change without notice

Information Canada
Ottawa, 1971

Design Criteria for Multi-Wire Borehole Extensometer Systems

by

D.G.F. Hedley*

Page

Effect of Anchors and Wires in a Borehole	1
Effect of Friction in the Extensometer	2
Sources of Friction	6
Methods of Reducing Friction	6
Effect of Friction Between Wire, Borehole and	
Anchors	8

ABSTRACT

The accuracy and limitations of a measuring system should be known before embarking on an instrumentation program. Errors in borehole extensometer measurements, their order of magnitude and methods of reducing or eliminating their influence, are presented in this paper. Also a method of calibrating extensometers in the laboratory, and a procedure for taking measurements in-situ are described.

The theoretical and practical investigations have indicated that extensometers with constant tension characteristics are potentially more accurate than those where the tension varies with the amount of wire movement. Friction in the extensometer and in the borehole, and change in temperature are considered to be the main sources of error. However, change in the physical properties and the sag of the wire can considerably affect the measurements with variable tension extensometers.

Coefficients of Linear Expansion	17
Error Due to Sag of the Wire	24

Extensometer: Error: Accuracy: Calibration

* Research Scientist, Mining Research Centre, Elliot Lake Laboratory, Mines Branch, Department of Energy, Mines and Resources, Elliot Lake, Ontario.

Crown Copyright Reserved.

CONTENTS

	<u>Page</u>
Abstract	i
1. Introduction	1
2. Factors Affecting the Accuracy of Extensometer Measurements	2
2.1 Friction	3
2.1.1 Friction in the Extensometer	3
2.1.2 Friction Between Wire and Borehole	7
2.1.3 Friction Between the Wire and Anchors	11
2.1.4 Friction Between the Wires	14
2.2 Change in Temperature	15
2.3 Change in Physical Properties of the Wire	18
2.4 Sag of the Wire	23
3. Laboratory Calibration of Extensometers	25
4. Procedure for In-Situ Reading of Extensometers	27
5. Conclusions	29

LIST OF FIGURES

	<u>Page</u>
1. Layout of Anchors and Wires in a Borehole	1
2. Effect of Friction in the Extensometer	4
3. Sources of Friction in Extensometers	6
4. Methods of Reducing Friction in Extensometers	6
5. Effect of Friction Between Wire, Borehole and Anchors	8
6. Maximum Unsupported Wire Length at Different Tensions	10
7. Diagrammatic Presentation of a Non-aligned Borehole ..	12
8. Effect of Temperature on Wire Length	16
9. Variation of Apparent Elastic Modulus with Applied Tension	20
10. Nomograph for Calculating Correction Factors for Variable Tension Extensometers	22
11. Calibration and Accuracy Curves for Constant Tension and Variable Tension Extensometers	26
12. Example of the Interpretation of Extensometer Measurements Using Two Tensions	29

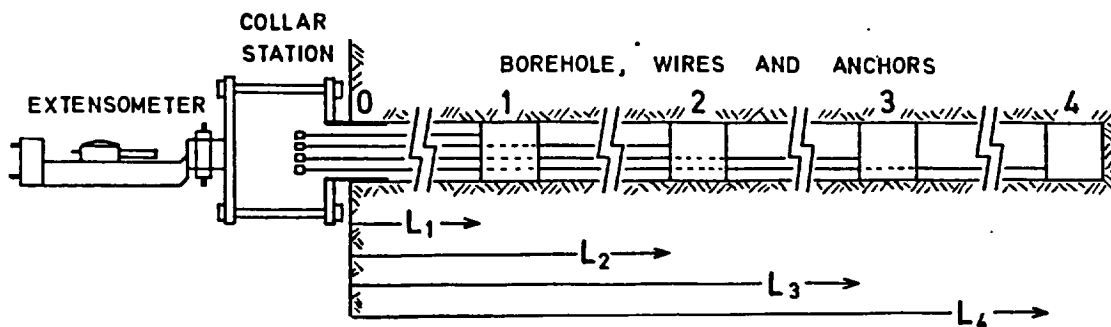
LIST OF TABLES

1. Coefficients of Linear Expansion	17
2. Error Due to Sag of the Wire	24

1. INTRODUCTION

One of the simplest methods of measuring rock-mass movements produced by mining, is with a borehole extensometer. The basic principle of the measuring system is to anchor one end of a wire at a predetermined depth in a borehole, and the other end to an extensometer at the borehole collar. Tension is applied to the wire through the extensometer and measurements are taken of the relative axial movement between the wire and the borehole. In other words, the length of the borehole is compared to a constant length of wire. Where more than one wire is installed, the intermediate anchors have holes drilled through them to allow free passage of the longer wires. In this way movement at different depths in the borehole can be evaluated.

The wires generally used are stainless steel, 0.030-inch or 0.049-inch diameter, or flexible stainless steel cable 0.019-inch diameter. The borehole anchors are set hydraulically. A typical layout of an extensometer borehole with anchors and wires is shown in Figure 1. Four anchors and wires are installed



	Movement	Strain
Wire L ₁	ΔL_1	$\epsilon_{0,1} = \frac{\Delta L_1}{L_1}$
Wire L ₂	ΔL_2	$\epsilon_{1,2} = \frac{\Delta L_2 - \Delta L_1}{L_2 - L_1}$
Wire L ₃	ΔL_3	$\epsilon_{2,3} = \frac{\Delta L_3 - \Delta L_2}{L_3 - L_2}$
Wire L ₄	ΔL_4	$\epsilon_{3,4} = \frac{\Delta L_4 - \Delta L_3}{L_4 - L_3}$

Figure 1: Layout of Anchors and Wires in a Borehole

at depths of L_1 , L_2 , L_3 and L_4 from the borehole collar. The axial strain between adjacent anchors is calculated as shown in Figure 1, and the strain rate is obtained by dividing the strain values by the time interval between each set of measurements.

Although this measuring system is basically simple there are a number of errors, such as those produced by friction and temperature changes, which can affect the measurements. If these errors are significant and not recognized then the measurements obtained are misleading.

Presented in this paper are:

- a) The sources of error associated with extensometer measurements, their likely order of magnitude and means of reducing or eliminating them.
- b) A method of calibrating extensometers in the laboratory.
- c) A procedure for taking measurements in-situ.

2. FACTORS AFFECTING THE ACCURACY OF EXTENSOMETER MEASUREMENTS

Extensometers are mainly used to measure two types of rock movement: that produced by change in stress, resulting in a relatively small deformation of the rock-mass; and that produced by fracturing, resulting in relatively large movements due to opening and sliding along cracks, faults and joints. Obviously the accuracy of the measurements needs to be greater in the first case than in the second.

The overall accuracy depends on the combined effect of individual errors in the measuring system. The factors which produce these errors are:

- a) Friction in the extensometer and between the wires, borehole and anchors.
- c) Change in temperature.
- c) Change in physical properties of the wire.
- d) Change in sag of the wire.

In some extensometer systems only a few of these factors affect the measurements, while in other systems all of these factors have an effect. In order to obtain an acceptable overall accuracy of measurement it is simpler to evaluate the magnitude of the individual errors and to devise means of reducing them. It is suggested that the overall error should not be more than .010 inch for measuring movement due to change in stress and not more than .050 inch for measuring movement due to fracturing of the rock. Therefore, the individual errors should not be more than .002 inch and .010 inch for the two types of rock movement. These arbitrarily chosen levels of accuracy are probably sufficient for the present and can be improved upon as the measuring techniques improve. As will be shown in the following sections, these accuracies are easily achieved for short measuring lengths. In this respect, the deformation due to change in stress is rarely measured in boreholes over 100 feet in length, whereas the movement of fractured rock is occasionally measured in boreholes up to 400 feet in length.

2.1 Friction

Tension applied to a wire through an extensometer is progressively reduced along its length due to the friction in the extensometer and between the wires, borehole and anchors. Consequently, the length of a wire is shorter than when a constant tension is applied along its complete length. This fact in itself is not important if it can be assumed that the friction remains constant. However, this may not be the case and it is expedient to evaluate the importance of the different frictional effects.

2.1.1 Friction in the Extensometer

Friction in the extensometer affects the whole wire length. The following example illustrates the order of magnitude of the error due to friction.

Friction in extensometer = F lb, assume = 1 lb
 Length of wire = L inches
 Diameter of wire = d inches
 Elastic modulus of wire = E psi, assume = 24×10^6 psi

Change in stress ' σ ' acting on the wire due to friction,

$$\sigma = \frac{F}{\frac{\pi}{4} d^2} \dots\dots\dots(\text{Eq. 1})$$

This produces a change ' ΔL ' in length of the wire where,

$$\Delta L = \frac{\sigma L}{E} = \frac{F}{\frac{\pi}{4} d^2} \frac{L}{E} = \frac{1}{\frac{\pi}{4} \times 24 \times 10^6} \times \frac{L}{d^2} \dots\dots\dots (\text{Eq. 2})$$

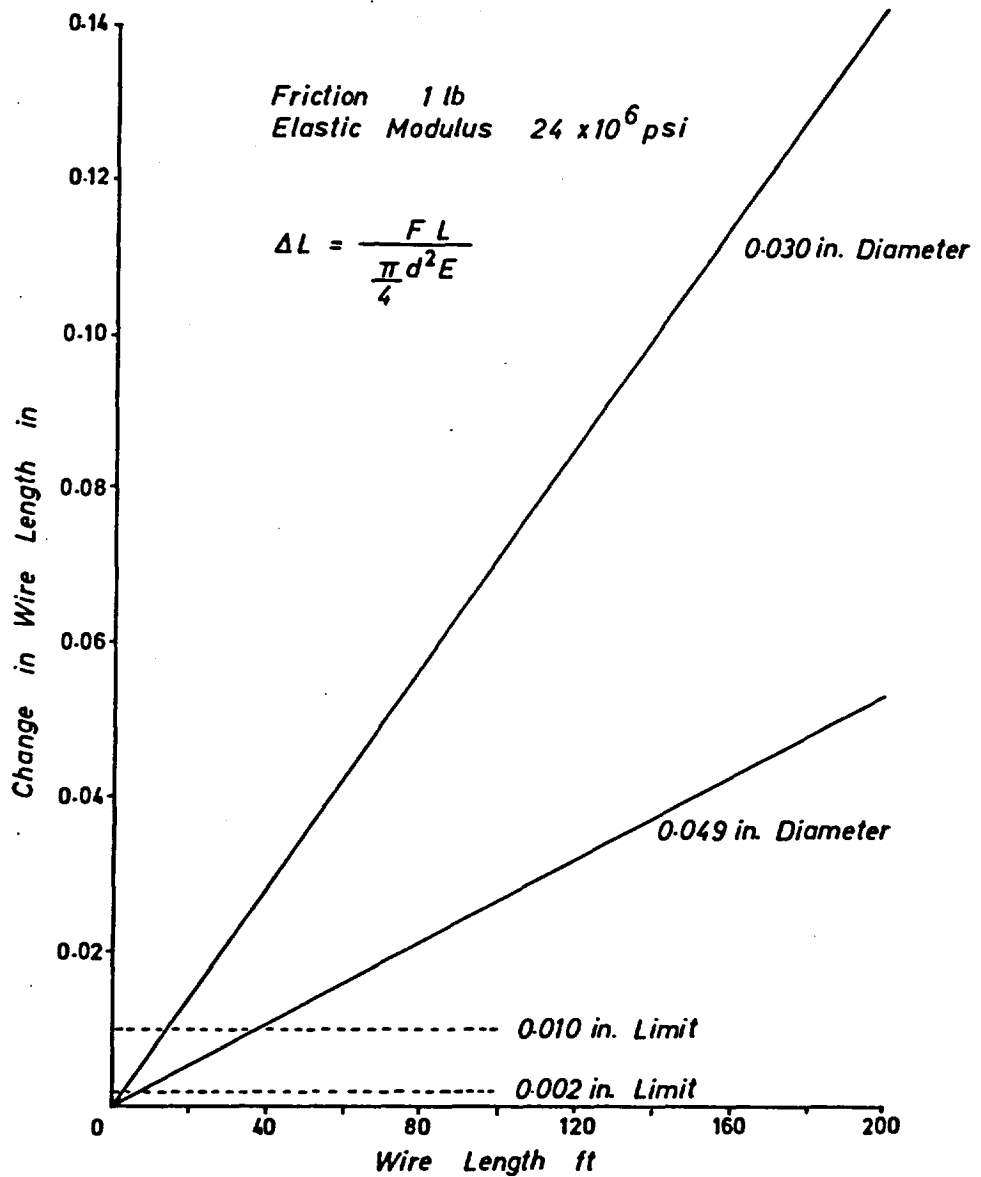


Figure 2: Effect of Friction in the Extensometer

Figure 2 is a graphical presentation of Equation 2, showing the change in wire length produced by a friction of 1 lb for wire lengths up to 200 feet and two wire diameters. This change in wire length is the error that would be produced if the friction changed by 1 lb between one reading and the next. The dotted lines in Figure 2 indicate the 0.010-inch and 0.002-inch error limits. The effect of 1-lb friction becomes significant for the upper limit at wire lengths of 15 feet and 38 feet, and for the lower limit at wire lengths of 3 feet and 7 feet for wire diameters 0.030 inch and 0.049 inch respectively.

This example clearly indicates that to obtain errors less than 0.010 inch for wire lengths over 38 feet the friction in the extensometer must be reduced well below 1 lb, and for errors less than 0.002 inch the friction must be almost eliminated. The effect of friction may be reduced by using a larger diameter wire, or by vibrating the extensometer to momentarily separate any sliding parts. However, neither of these methods gets at the source of the problem. The best method of reducing friction is in the design of the extensometer.

There are usually two separate measuring systems incorporated in an extensometer: one measures tension applied to the wire, and the other measures wire movement. Some common methods of applying tension are through a compression or extension helical spring, a cantilever, a dead weight, a NEG'ATOR* constant-tension spring, and a NEG'ATOR constant-torque spring. A dial gauge or vernier is used to measure deflection of helical springs, and strain gauges to measure cantilever deflection. Wire movement can be measured with a dial gauge, a micrometer, a precision screw thread, or electrical transducers for remote readout. Some extensometers incorporate the spring and wire movement in one measurement. This necessitates a knowledge of the spring constant (i.e. lbs exerted per inch deflection), and the elastic modulus of the wire, so that the two movements can be separated. The method of doing this is given in Section 2.3.

Most of the friction in extensometers is developed by guides for helical springs, and tie bars sliding through bearings. Figures 3(a), (b) and (c) show three tensioning devices where friction can significantly affect the measurement. In (a) friction is produced between the piston and tube surrounding the compression spring. In (b) friction is produced between the sleeves on the spring balance and also between the tie rods and

* Hunter Spring Co. Trademark.

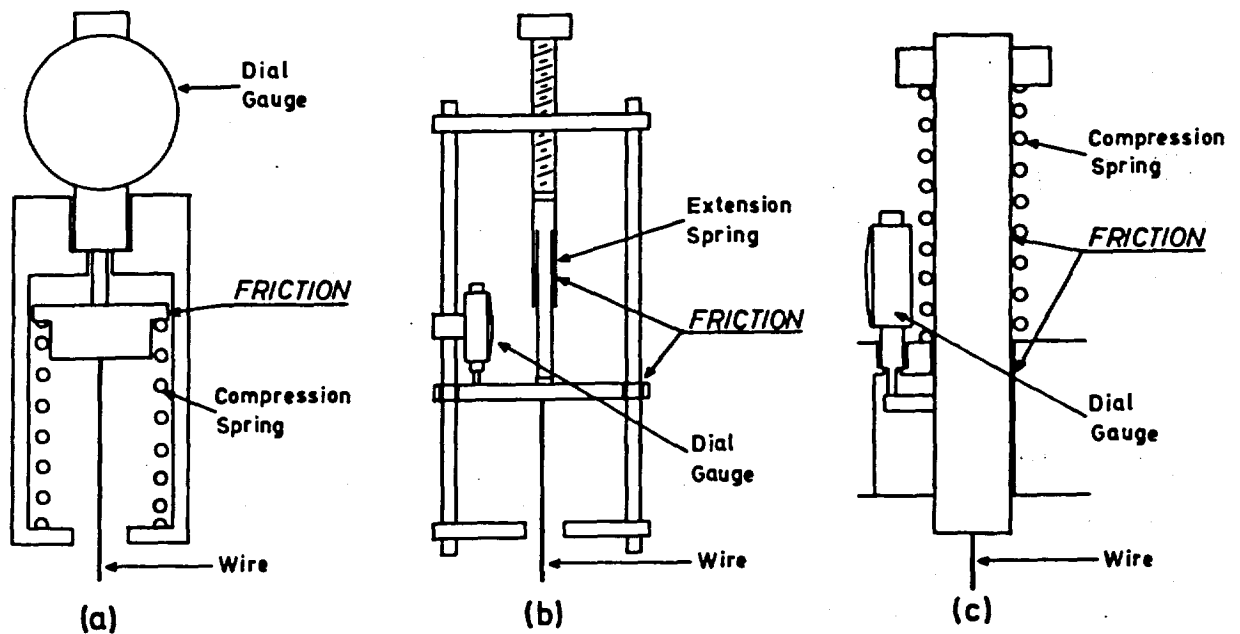


Figure 3 : Sources of Friction in Extensometers

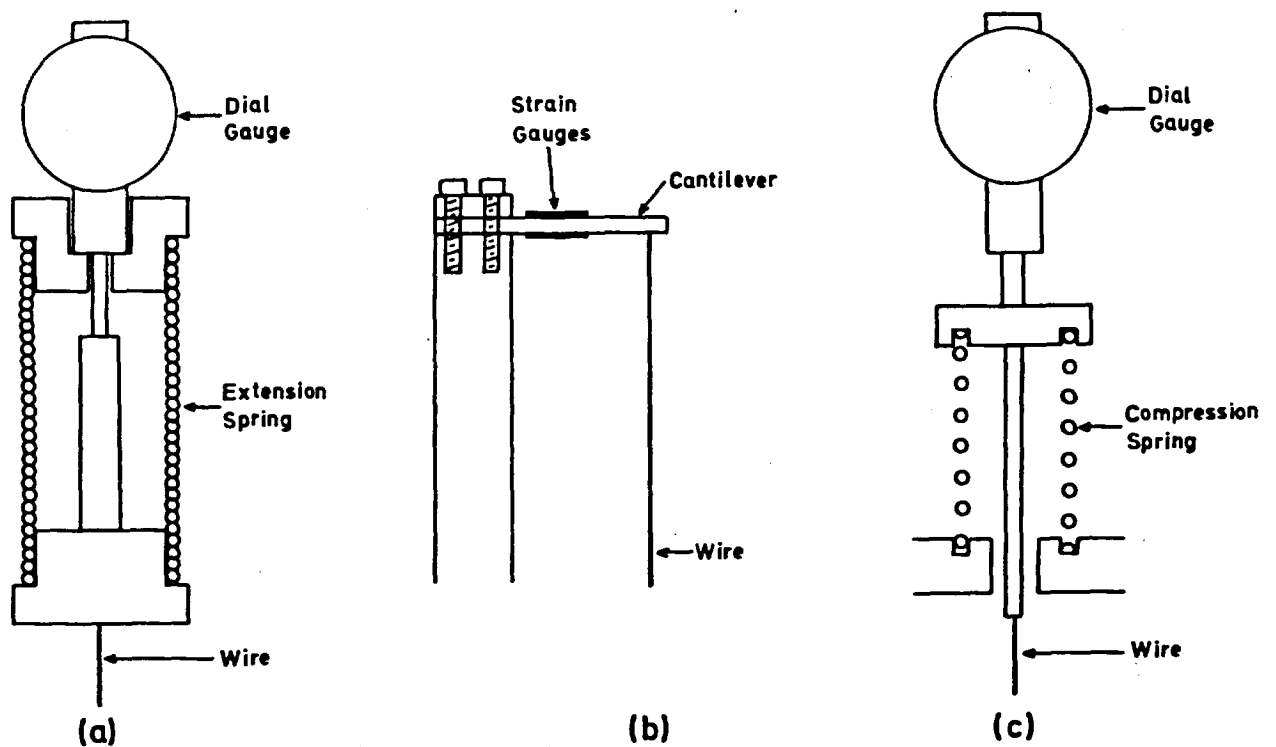


Figure 4 : Methods of Reducing Friction in Extensometers

sliding plate. In (c) friction is produced between the tie bar and the compression spring and between the tie bar and housing. Also where the length to diameter ratio of a compression spring is greater than 4:1 the spring has a tendency to buckle, resulting in excessive friction.

Figures 4(a), (b) and (c) show three tensioning device designs where there is no friction. One method of eliminating friction is by using extension springs which do not require guides, as shown in Figure 4(a). A cantilever with electrical strain gauges to measure deflection is shown in Figure 4(b). Compression springs can be used if they have a relatively large diameter, and are compressed by an internal rod which is neither in contact with the spring nor housing, as shown in Figure 4(c). All tensioning devices should be connected directly to the wire. Consequently, any friction developed in the rest of the extensometer only affects the length of the extensometer body which is much larger than the wire and the effect is negligible.

Using the principles outlined it should be possible to design an extensometer in which friction does not significantly affect the measurements. Other errors, such as backlash in gears, have to be evaluated by calibrating the extensometer in the laboratory and one method of testing is described in Section 3.

2.1.2 Friction between Wire and Borehole

Where the surface of the wire and borehole are in contact there is a limited amount of resistance (friction) to sliding. The force 'F' necessary to overcome this resistance is,

$$F = \mu N \dots\dots\dots(\text{Eq. 3})$$

where, μ = coefficient of static friction,
N = force normal to the contact surface.

The force N is the weight of the wire supported by the borehole.

The following example illustrates the effect of borehole friction on wire length.

Length of wire supported by borehole	= L inches
Diameter of wire	= d inches
Elastic modulus of wire	= E psi = 24×10^6 psi
Density of wire	= λ = .28 lb/cu in (stainless steel)
Coefficient of friction, steel on rock	= μ , assume = 0.5

Weight N supported by borehole = $L \times \frac{\pi}{4} d^2 \times \lambda$.

Friction $F = \mu \times L \times \frac{\pi}{4} d^2 \times \lambda$.

Decrease in stress σ in the wire due to friction,

$$\sigma = \frac{F}{\frac{\pi}{4} d^2} = \frac{\mu \times L \times \frac{\pi}{4} d^2 \times \lambda}{\frac{\pi}{4} d^2} = \mu \times L \times \lambda$$

Although the friction acts along the whole length of the wire, for the purpose of calculation, it can be assumed that it is concentrated at the mid-point of the wire. Therefore half the length of wire is subjected to an average stress σ less than the other half, which produces a reduction in wire extension ΔL .

$$\Delta L = \frac{\sigma}{E} \frac{L}{2} = \frac{\mu \lambda L^2}{2E} = \frac{0.5 \times .28}{2 \times 24 \times 10^6} L^2 \dots\dots (Eq. 4)$$

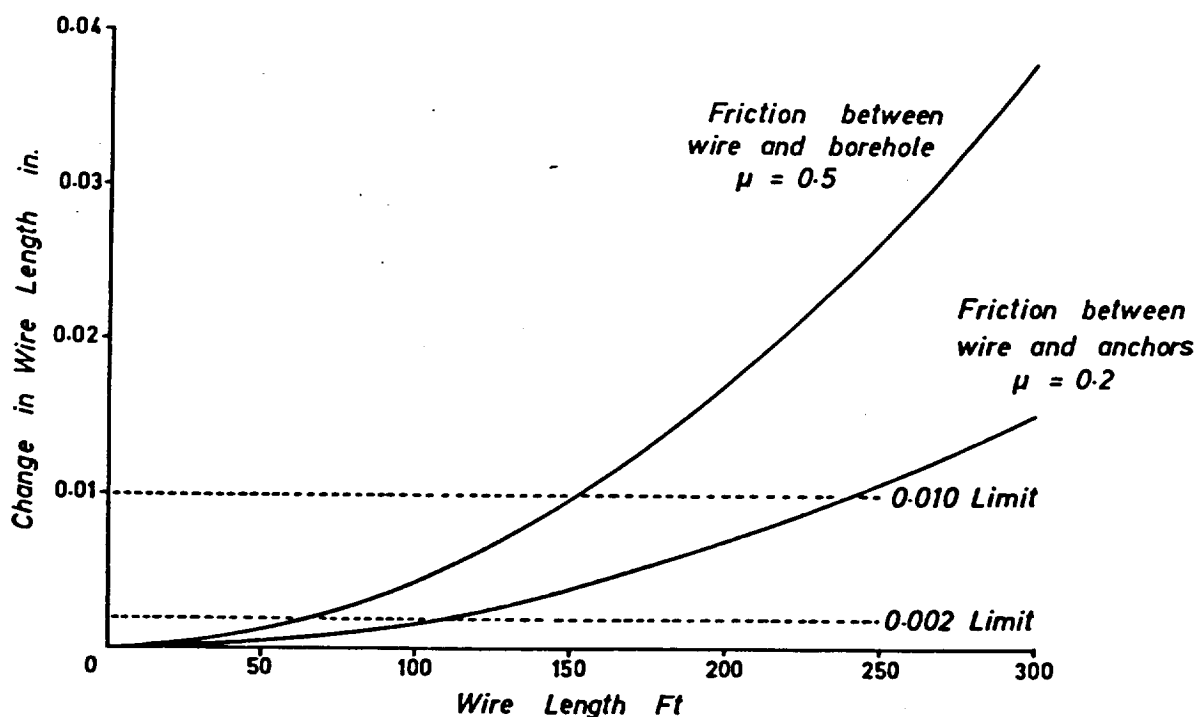


Figure 5 : Effect of Friction between Wire, Borehole and Anchors

Figure 5 is a graphical presentation of Equation 4, showing the reduction in wire extension for wire lengths up to 300 feet and represents the maximum error that can be produced by the friction between the wire and the borehole. The dotted lines in Figure 5, again represent the .010-inch and .002-inch error limits. In this case the effect of friction becomes significant at a wire length of 154 feet for the upper limit and 69 feet for the lower limit. Changing the wire diameter has no effect on the magnitude of the error.

The contact between the wire and borehole can be reduced or eliminated by increasing the tension applied to the wire or by reducing the distance between anchors. In a horizontal borehole the wires are suspended between adjacent anchors or an anchor and the extensometer. The curve of equilibrium (catenary curve) assumed by a flexible wire can be represented by,

$$y = \frac{qx^2}{2H} \dots\dots\dots(\text{Eq. 5})$$

where, y = vertical displacement of the wire relative to its lowest point,
 x = horizontal distance from the lowest point,
 H = applied horizontal tension,
 q = weight per unit length of wire.

Also,

$$x = \frac{L}{2} = \sqrt{\frac{2y'H}{\frac{\pi}{4} d^2 \lambda}} \dots\dots\dots(\text{Eq. 6})$$

where, y' = maximum vertical displacement,
 L = total length of wire,
 d = wire diameter,
 λ = density of wire ($\frac{\pi}{4} d^2 \lambda = q$).

Boreholes are usually confined to four sizes, EX, AX, BX and NX of diameters 1.48, 1.89, 2.36 and 2.98 inches. If the ends of the wire are located in the centre of the borehole, then the maximum permissible sag is half the borehole diameter. A graphical presentation of Equation 6 is shown in Figure 6. This graph relates maximum length of unsupported wire, for different tensions, borehole sizes and two wire diameters. The graph shows that the length of unsupported wire in a borehole increases with increasing tension and decreasing wire diameter. There is a limit to the amount of tension that can be applied to a wire, the yield strength of stainless steel is approximately 36 lb for 0.030-inch diameter and 100 lb for 0.049-inch diameter. Most extensometers can apply tension between 0 and 30 lb.

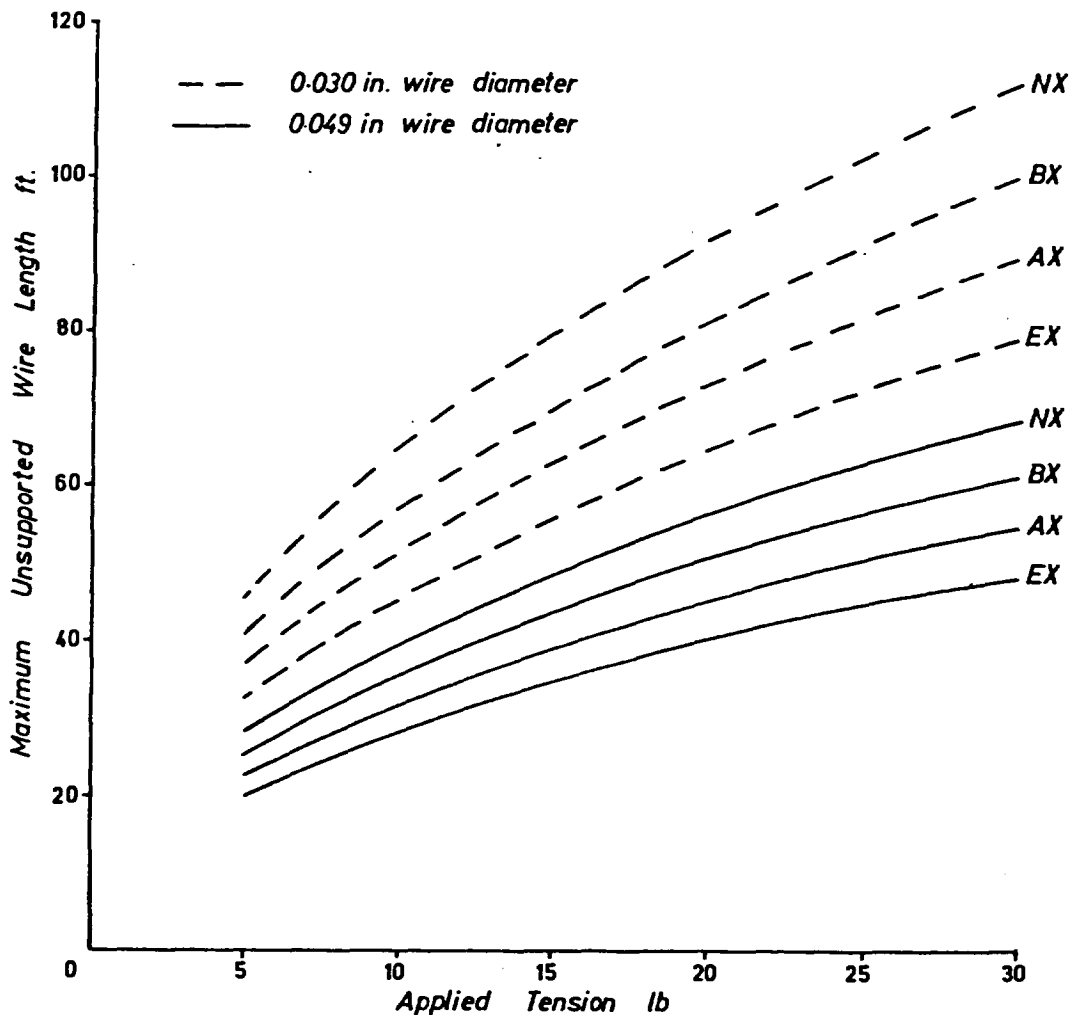


Figure 6 : Maximum Unsupported Wire Length at Different Tensions

Figure 6 can be used to determine the tension, wire diameter and interval of supports which prevents contact between the wire and borehole. For instance, a 100-foot wire in an AX borehole at 20-lb tension requires one support for 0.030-inch diameter wire and two supports for 0.049-inch diameter wire, while a 400-foot wire requires five and eight equally spaced supports for the same wire diameters. This graph is only applicable for horizontal boreholes. Sag of the wire, perpendicular to the axis of the borehole, reduces as the inclination of the borehole increases. Ultimately for vertical boreholes there is no sag.

Although the methods outlined reduce or eliminate the friction between the wire and borehole this transfers the friction to between the wire and anchors or supports, which is discussed in the following sub-section.

2.1.3 Friction Between the Wire and Anchors

The total weight of the wire, provided it is not in contact with the borehole, is supported by the anchors and extensometer. The wire sliding over the anchors will produce friction and the effect on wire length can be calculated using Equation 4, except in this case the coefficient of friction (metal on metal) will be approximately 0.2.

Therefore,

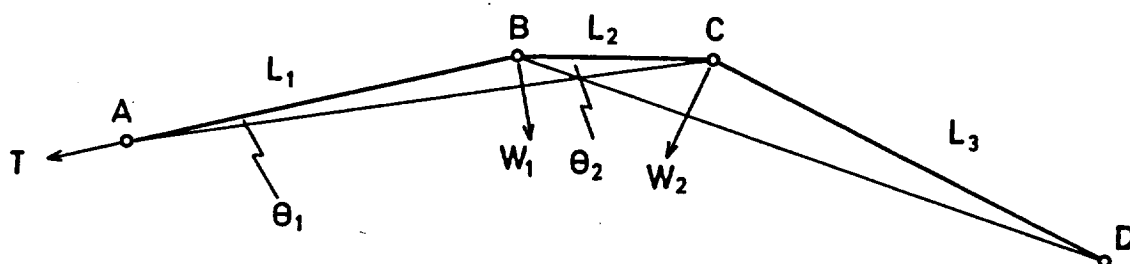
$$\Delta L = \frac{0.2 \times .28}{2 \times 24 \times 10^6} L^2 \dots\dots\dots (\text{Eq. 4a})$$

Equation 4a is graphically presented in Figure 5, with Equation 4.

In this case the effect of friction becomes significant at a wire length of 244 feet for the upper limit and 109 feet for the lower limit. Since small movements due to change in stress are rarely made over 100 feet, the effect of friction is acceptable. To reduce the friction in longer lengths of wire the easiest method is to reduce the coefficient of friction. Teflon* bearings in the anchors would reduce the coefficient of friction to 0.04. Consequently, the wire length for the upper limit now becomes 545 feet and for the lower limit 244 feet.

* DuPont trademark.

When the borehole is not straight, friction between the wire and anchors may become important. If the extensometer, intermediate anchors and end anchor are not in a straight line, a component of the applied tension is transmitted to the intermediate anchors. The same result occurs where there are no intermediate anchors and the wire transmits part of the tension to the side of the borehole.



ABCD represents a wire in a borehole,

- A represents the extensometer,
- B represents the first anchor,
- C represents the second anchor,
- D represents the last anchor,
- T = tension applied by extensometer,
- W_1 = component of tension applied to point B,
- W_2 = component of tension applied to point C,
- θ_1 = angle subtended by points BAC,
- θ_2 = angle subtended by points CBD,
- L_1 = wire length A to B,
- L_2 = wire length B to C,
- L_3 = wire length C to D,
- L = total length = $L_1 + L_2 + L_3$.

Figure 7: Diagrammatic Presentation of a Non-aligned Borehole

The effect of friction due to non-alignment of the borehole is shown in the following example. In Figure 7, the friction F_1 produced at B due to the component of the applied tension and the weight of the wire is,

$$F_1 = \mu T \sin \theta_1 + \frac{\mu}{2} (L_1 + L_2) \frac{\pi}{4} d^2 \lambda \quad \dots \dots (\text{Eq. 7})$$

and similarly friction F_2 at C is,

$$F_2 = \mu T \sin \theta_2 - \mu^2 T \sin \theta_1 \sin \theta_2 - \frac{\mu^2}{2} \sin \theta_2 (L_1 + L_2) \frac{\pi}{4} d^2 \lambda \\ + \frac{\mu}{2} (L_2 + L_3) \frac{\pi}{4} d^2 \lambda \dots\dots\dots (\text{Eq. 8})$$

where μ = coefficient of friction,
 d = wire diameter,
 λ = wire density.

In Equation 8, the terms involving μ^2 are much smaller than those involving μ , and the former can be neglected. Consequently,

$$F_2 \approx \mu T \sin \theta_2 + \frac{\mu}{2} (L_2 + L_3) \frac{\pi}{4} d^2 \lambda \dots\dots (\text{Eq. 8a})$$

If point D moves, then before movement is transmitted to length L_2 the friction at point C has to be overcome which produces a change in length $\Delta L'$ of L_3 , where,

$$\Delta L' = \frac{L_3}{\frac{\pi}{4} d^2 E} \left(\mu T \sin \theta_2 + \frac{\mu}{2} (L_2 + L_3) \frac{\pi}{4} d^2 \lambda \right) \dots\dots (\text{Eq. 9})$$

where, E = elastic modulus of the wire.

Before movement is transmitted to L_1 and the extensometer, friction at B has to be overcome, resulting in a further change in length $\Delta L''$ of L_2 and L_3 , where,

$$\Delta L'' = \frac{L_2 + L_3}{\frac{\pi}{4} d^2 E} \left(\mu T \sin \theta_1 + \frac{\mu}{2} (L_1 + L_2) \frac{\pi}{4} d^2 \lambda \right) \dots\dots (\text{Eq. 10})$$

The total change in length ΔL is obtained by adding Equations 9 and 10.

$$\Delta L = \frac{\mu T}{\frac{\pi}{4} d^2 E} (L_3 \sin \theta_2 + (L_2 + L_3) \sin \theta_1) + \frac{\mu \lambda}{2E} (L - L_1) L \dots (\text{Eq. 11})$$

Consequently, provided the profile of the borehole is known the frictional effects for any combination of tension, wire length and diameter can be calculated. In a special case where $\theta_1 = \theta_2$ and $L_1 = L_2 = L_3 = \frac{L}{3}$ Equation 11 simplifies to,

$$\Delta L = \frac{\mu L}{E} \left[\frac{T \sin \theta_1}{\frac{\pi}{4} d^2} + \frac{\lambda L}{3} \right] \dots \dots \dots (\text{Eq. 11a})$$

when, for example, $\mu = .04$, teflon to steel,
 $E = 24 \times 10^6$ psi,
 $T = 20$ lb,
 $\theta = 5^\circ$,
 $d = .048$ inch,
 $\lambda = .28$ lb/ cu in.

then ΔL for a 100-foot wire is .002 inch and for a 400-foot wire it is .011 inch. These are acceptable errors, but it emphasizes the need to have low-friction bearings to support the wire.

2.1.4 Friction Between the Wires

In multi-wire boreholes it is often observed that if one wire is pulled the other wires tend to move as well. This is due to the wires being intertwined, partly caused by the natural curvature of the wire. The tension applied to one wire is partially transmitted to other wires. In an extreme case the wires would behave as a wire rope.

It is impossible to theoretically calculate the effect of intertwining of wires on the accuracy of the measurements, other than to say the effects are likely to be large. Therefore, it is advisable to eliminate all contact between the wires, by having a separate hole in the anchors for each wire and, if necessary, spacers between anchors. At present, a maximum of five wires are installed in an AX borehole (1.89-inches diameter) and usually only four. When readings are being taken on one wire, if the other wires have small tensions applied to them, this would tend to straighten the wires and keep them out of contact. It is important that anchors and wires be installed in a borehole without any rotational movement, otherwise the wires will be twisted.

2.2 Change in Temperature

To obtain the true movement of a borehole, correction factors must be applied to compensate for the change in length of the borehole and wire, due to change in temperature. Underground the change in borehole temperature is usually minimal, except where the boreholes are situated in intake airways. Boreholes drilled from the surface will be subjected to seasonal temperature variations. Closed-end boreholes will be affected to a depth of approximately 25 feet (perpendicular to the surface), below which the temperature remains reasonably constant. Open boreholes will be affected over their complete length due to natural ventilation.

The error produced by change in temperature can be calculated, using

$$\Delta L = LT\beta \quad \dots\dots\dots(\text{Eq. 12})$$

where,

ΔL = error,
 L = wire length,
 T = change in temperature,
 β = difference between wire and rock coefficients of linear expansion.

Figure 3 shows a graphical presentation of Equation 12. A 10°F change in temperature on a 200-foot wire with a difference in coefficient of linear expansion of $2 \times 10^{-6}/^{\circ}\text{F}$ will produce an error of .048 inch. If the wire coefficient of linear expansion is greater than that of the rock, for an increase in temperature the measurements will show an apparent borehole shortening, and if the rock coefficient is greater the measurements will show an apparent borehole lengthening. The coefficients of linear expansion for some common types of rock and stainless steel wires are given in Table 1.

To reduce the temperature error, the coefficients of linear expansion of the rock and wire should be matched as far as possible. Table 1 shows that in general, the coefficients of linear expansion of stainless steel wires are greater than those for the common types of rocks. Certain nickel-iron alloys, such as invar, have very low coefficients of linear expansion and it may be possible to use these alloys for rocks with low coefficients. These arguments assume that the rock mass is free to expand with increasing temperature. However, if the rock is constrained then thermal stresses will be induced.

*Difference between Wire and Rock Coefficients
of Linear Expansion $\times 10^{-6}/^{\circ}F$*

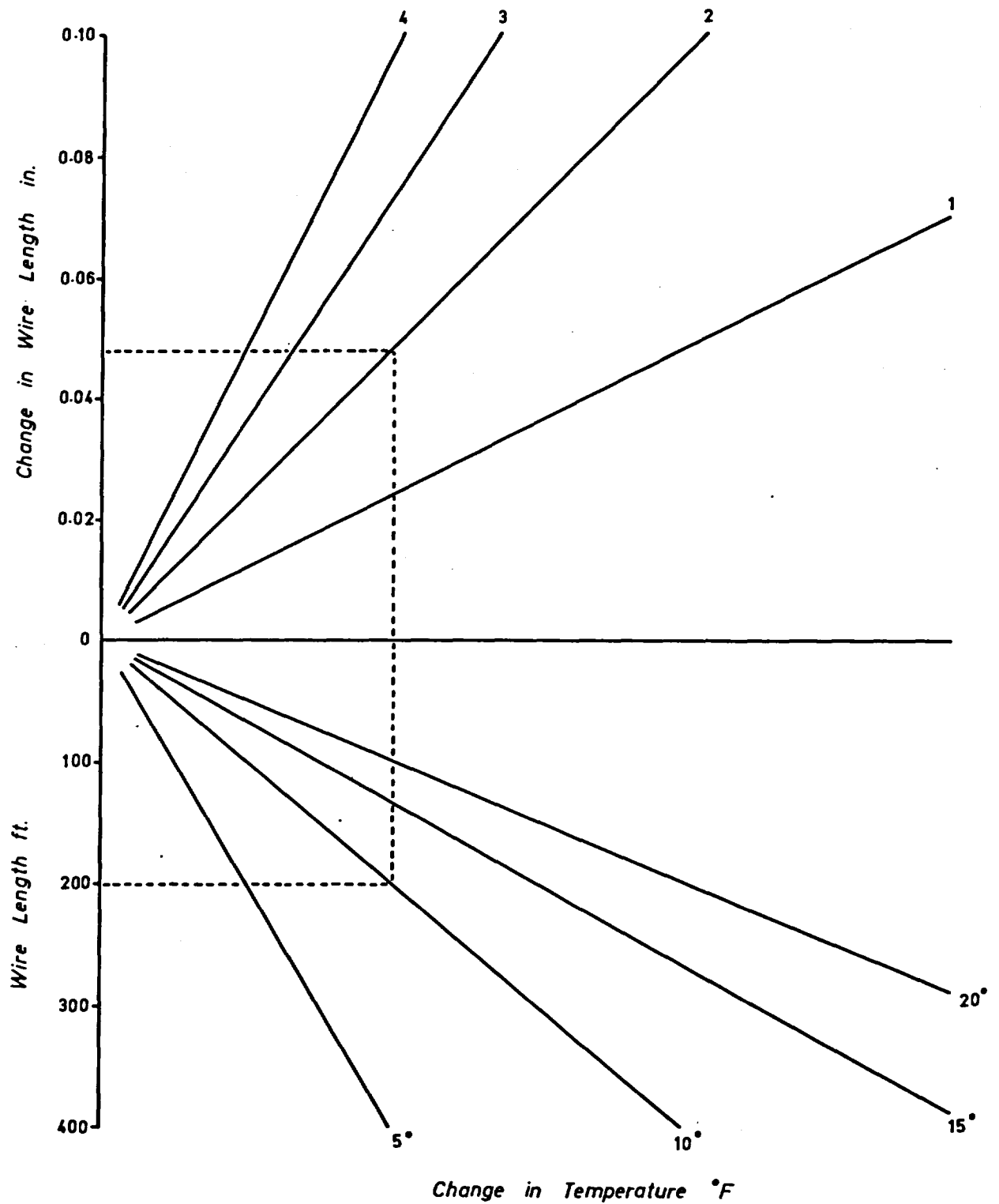


Figure 8: Effect of Temperature on Wire Length

TABLE 1
Coefficients of Linear Expansion

Rocks*	Mean Coefficient of Linear Expansion $\times 10^{-6}/^{\circ}\text{F}$
Granites and rhyolites	4.5
Andesites and diorites	4.0
Basalts, gabbros and diabases	3.0
Sandstones	5.5
Quartzites	6.0
Limestones	4.5
Marbles	4.0
Slates	5.0
Salt and potash	21
Stainless Steels	
AISI ⁺ 446 27% Cr	5.5
AISI 403 12% Cr	6.1
AISI 420 12% Cr over .15% C	6.8
AISI 310 25% Cr 20% Ni	3.5
AISI 305 13% Cr 12% Ni	9.5
Invar 65% Fe 36% Ni	1.0

* From Handbook of Physical Constants, S.P. Clark, Jr. (Editor), Geological Society of America.

+ American Iron and Steel Institute.

In closed boreholes the effect of temperature in the first 25 feet of wire can be compensated for by installing a wire at this depth. The apparent movement measured on this wire is subtracted from the movements measured on the other wires. Consequently, the reference points for the measurements would be transferred from the collar of the borehole to a depth of 25 feet. Open boreholes, where the temperature variation may well be in the order of 30-60°F, should be plugged at one end to stop the natural ventilation, after which they will be affected to a depth of only 25 feet.

The total movement of the borehole, including temperature effects, can be measured by installing two wires, with different coefficients of linear expansion, at each anchor. The method of calculating total borehole movement is,

$$\text{first wire, } y_1 = LT\alpha_1 + x \text{(Eq. 13)}$$

$$\text{second wire, } y_2 = LT\alpha_2 + x \text{(Eq. 13a)}$$

where, y_1 and y_2 = measured movement on first and second wires,
 x = total movement of the borehole,
 α_1 and α_2 = coefficients of linear expansion of first and second wires,
 L = wire length,
 T = change in temperature.

These equations can be combined to

$$x = \frac{\alpha_2 y_1 - \alpha_1 y_2}{(\alpha_2 - \alpha_1)} \text{(Eq. 14)}$$

If the first wire is stainless steel ($\alpha_1 = 8.5 \times 10^{-6}/^{\circ}\text{F}$) and the second wire is Invar ($\alpha_2 = 1.0 \times 10^{-6}/^{\circ}\text{F}$) Equation 14 becomes

$$x = \frac{1}{7.5} (8.5 y_2 - y_1) \text{(Eq. 14a)}$$

Consequently, a knowledge of the actual change in temperature is not required to calculate the movement. This method of temperature compensation reduces the number of measurements, since to avoid wire interference only four or five wires can usually be installed in one borehole.

2.3 Change in Physical Properties of the Wire

Stainless steel is usually considered to have a constant elastic modulus of 28 to 30 x 10⁶ psi. However, this is not the case for stainless steel wire, which is usually supplied by the manufacturer in coils. At low tensions part of the apparent

stretch of the wire is the straightening of the natural curves of the wire which results in an apparent lower elastic modulus. Figures 9(a), (b) and (c) show the results of laboratory tests on a 64-foot length of 0.049-inch- and 0.030-inch-diameter stainless-steel wire, and 0.018-inch-diameter stainless-steel cable. Tests were performed on the solid wires, both in the as-received coiled condition, and after they had been pulled through a wire straightener. This straightener consists of two sets of nine pulleys mounted at 90 degrees to each other.

Figure 9(a) shows the results for the 0.049-inch-diameter wire. In the coiled condition at a tension of 4 lb the apparent elastic modulus is 8×10^6 psi. The modulus increases with increasing tension until above 15 lb it appears to reach an asymptotic value of 24×10^6 psi. After using the wire straightener the elastic modulus was approximately constant at 24×10^6 psi over the range tested (4 lb to 30 lb). The results for the 0.030-inch-diameter wire, Figure 9(b), were almost identical for both the coiled and straightened wire, with an apparent elastic modulus of 24×10^6 psi. Tests on the 0.018-inch nominal-diameter flexible cable, Figure 9(c), indicate that between tensions of 4 lb to 14 lb the apparent elastic modulus increase from 10×10^6 psi to 11×10^6 psi. In addition the moduli on the loading cycle are different from those on the unloading cycle.

These results indicate only constant-tension extensometers can be used with flexible stainless-steel cable. For solid stainless-steel wires, those with relatively large diameters should be straightened on site before being installed in a borehole. Alternatively, the initial tension applied to a wire should be sufficient to produce a constant elastic modulus. The minimum tension that should be applied can be estimated from the laboratory tests. Taking values of 15 lb and 5 lb for the 0.049-inch- and 0.030-inch-diameter wires gives applied stress values of 3000 psi and 7000 psi. Therefore, taking a slightly higher minimum stress value of 10,000 psi produces the following minimum tension values for wires of different diameters:

Wire Diameter inch.	Minimum Applied Tension lb
0.020	3
0.030	7
0.040	13
0.050	20
0.060	28

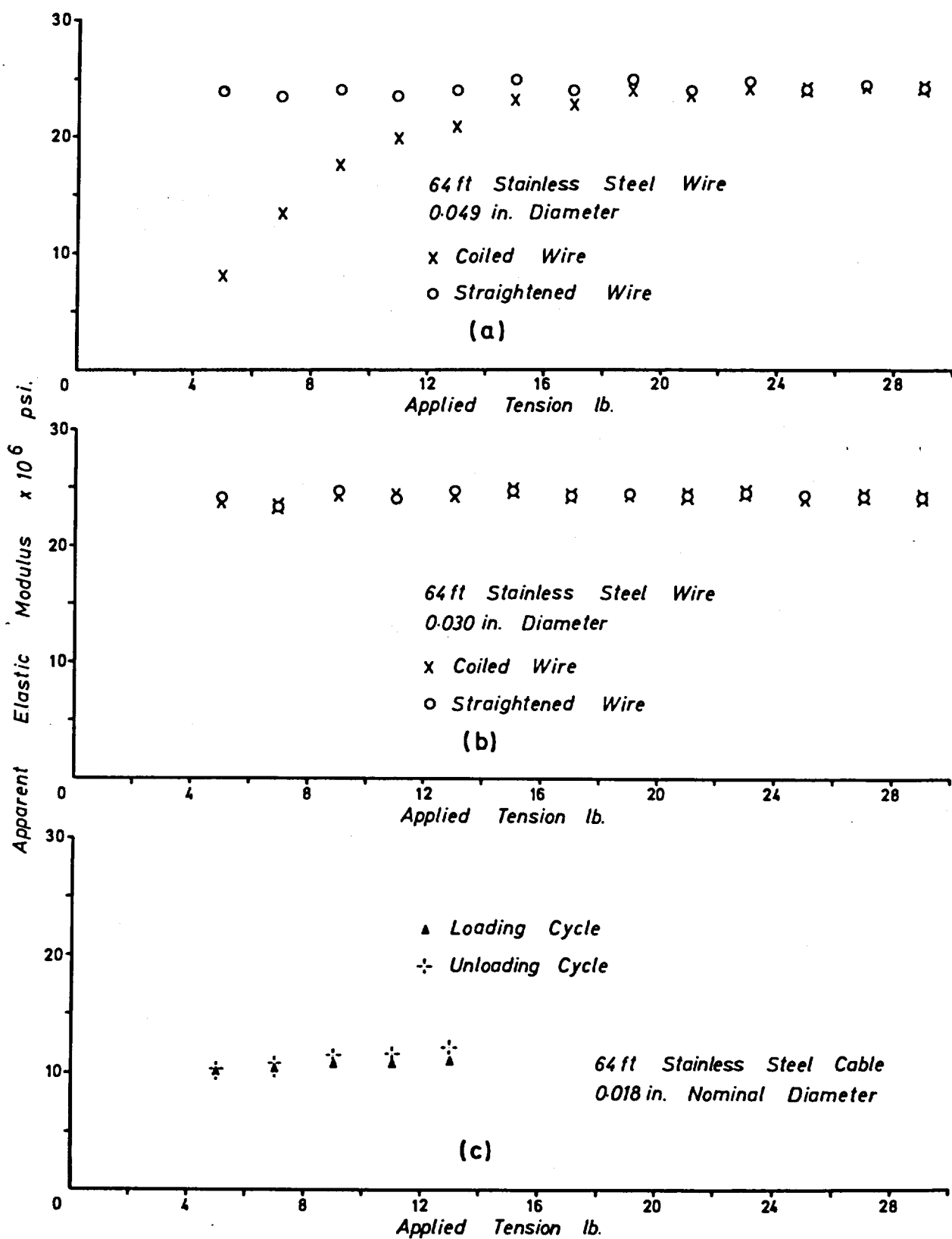


Figure 9: Variation of Apparent Elastic Modulus with Applied Tension

The variation in elastic modulus does not affect extensometers which apply a constant tension, but only those where tension alters with wire movement. In these instruments the measured movement is a combination of the movement of the wire minus the change in wire stretch. The true movement can be calculated using the following equation:

$$x = y \left[1 + \frac{CL}{\frac{\pi}{4} d^2 E} \right] \dots\dots\dots (\text{Eq. 15})$$

where, x = true movement (inches),
 y = measured movement (inches),
 C = spring constant (lb/in deflection),
 L = wire length (inches),
 d = wire diameter (inches),
 E = elastic modulus of wire (lb/sq in).

The term in the brackets is usually referred to as the correction factor.

Figure 10 shows a nomograph relating wire length, spring constant, wire diameter, elastic modulus and correction factor. The error produced by variation in elastic modulus is illustrated in the following example. Suppose that the elastic modulus was assumed to be 24×10^5 psi and that at the start of the measurements it was actually 16×10^5 psi. Then for a 100-foot wire, spring constant 10 lb/in and wire diameter 0.049 inch the correction factor applied to the measurement would be 1.264, whereas the actual correction factor should be 1.398. This produces an error of 10.6% in the initial movement measured on the wire. This example clearly illustrates the necessity of either straightening the wire or using tensions at which the elastic modulus is constant.

There is little information in the literature on the creep properties of stainless-steel wires at room temperature. Most of the information concerns high temperatures (1000°F) and at stresses approaching the yield point. Since maximum stresses of about 50,000 psi are applied to extensometer wires, and the yield point of 310 stainless steel is about 185,000 psi, creep is not considered an important source of error.

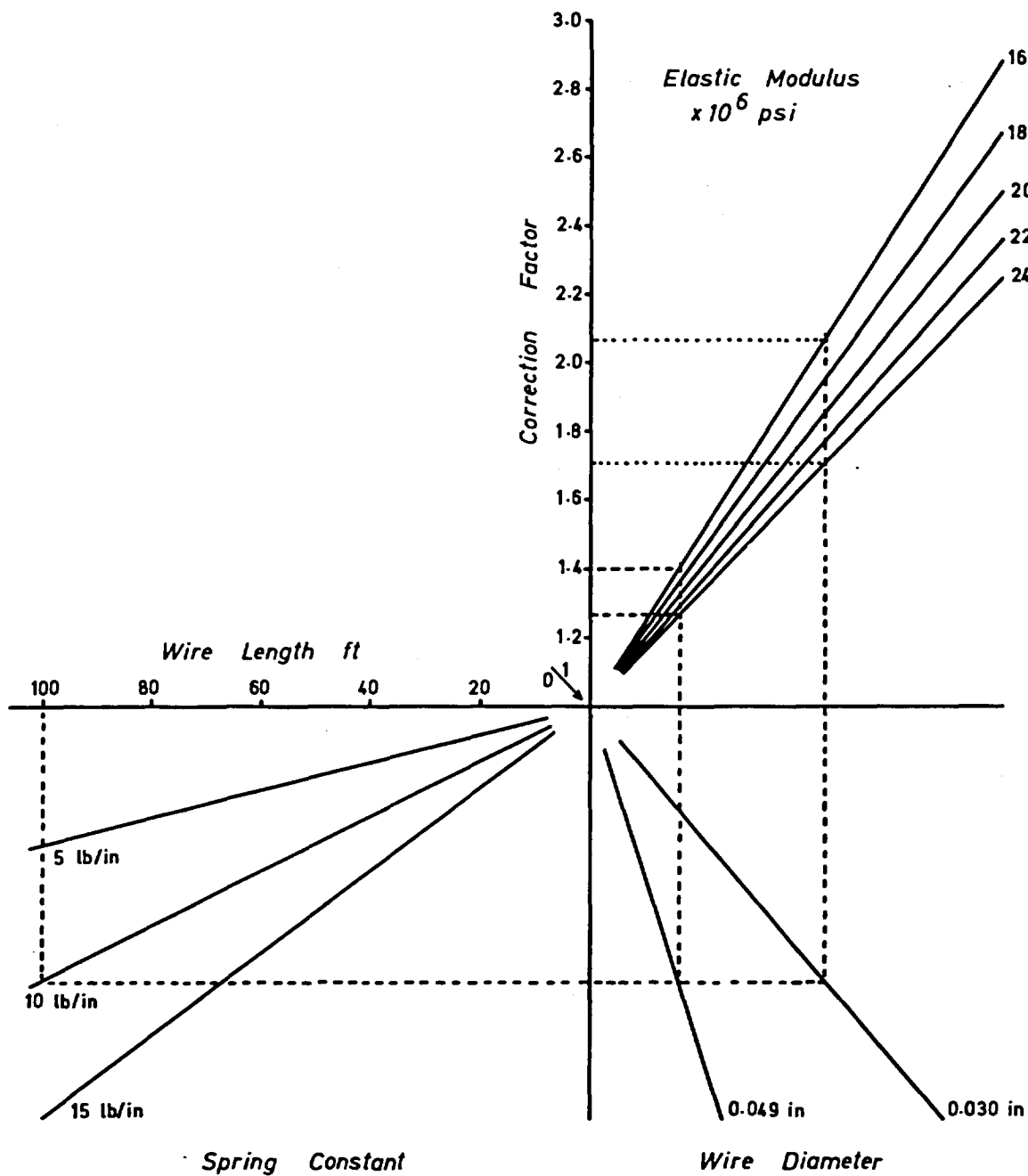


Figure 10: Nomograph for Calculating Correction Factors for Variable-Tension Extensometers

2.4 Sag of the Wire

As mentioned previously (Section 2.1.2) a wire suspended between two horizontal points hangs in a catenary curve. The horizontal distance between the two end points is less than the length of the wire. As the tension is increased the sag of the wire reduces and its length approaches the same value as the horizontal distance. This error does not affect constant-tension extensometers, since sag of the wire is always the same. However, variable-tension extensometers do produce a change in sag of the wire, and the methods of calculating this error are as follows.

For single suspended length,

$$\Delta L = \frac{q^2 l^3}{24} \left(\frac{1}{T_1^2} - \frac{1}{T_2^2} \right) \dots \dots \dots (\text{Eq. 16})$$

For uniformly spaced supports,

$$\Delta L = \frac{Lq^2 l^2}{24} \left(\frac{1}{T_1^2} - \frac{1}{T_2^2} \right) \dots \dots \dots (\text{Eq. 17})$$

where, ΔL = error,
 l = distance between support,
 L = total wire length,
 q = weight per unit length of wire,
 T_1 = initial tension,
 T_2 = final tension.

This error due to change in sag is complicated by the fact that the wires are in contact with the borehole and consequently are not freely supported. However, an estimate of the freely supported length can be obtained from the catenary equations by calculating the maximum length which does not touch the boreholes, for a particular tension and borehole size.

The following example illustrates the order of magnitude of the error due to sag.

	<u>1st Case</u>	<u>2nd Case</u>
Wire length	100 feet unsupported	100 feet supported at 25-foot intervals
Wire diameter	0.049 inch	0.049 inch
Wire weight	5.3×10^{-4} lb/in	5.3×10^{-4} lb/in
Max. deflection	1 inch	1 inch

Table 2 gives the incremental error for every 2-lb increase in tension between 2 lb to 30 lb, also the cumulative error is tabulated.

TABLE 2
Error Due to Sag of the Wire

Tension (lb)	100 feet unsupported		100 feet supported 25-foot intervals	
	Incremental error (inch)	Cumulative error (inch)	Incremental error (inch)	Cumulative error (inch)
2	.0045		.0462	
4	.0020	.0045	.0242	.0462
6	.0012	.0065	.0154	.0704
8	.0008	.0077	.0071	.0858
10	.0006	.0085	.0039	.0929
12	.0005	.0091	.0023	.0968
14	.0004	.0096	.0015	.0991
16	.0003	.0100	.0010	.1006
18	.0003	.0103	.0007	.1016
20	.0002	.0106	.0005	.1023
22	.0002	.0108	.0004	.1028
24	.0002	.0110	.0003	.1032
26	.0001	.0112	.0003	.1035
28	.0001	.0113	.0002	.1038
30		.0114		.1040

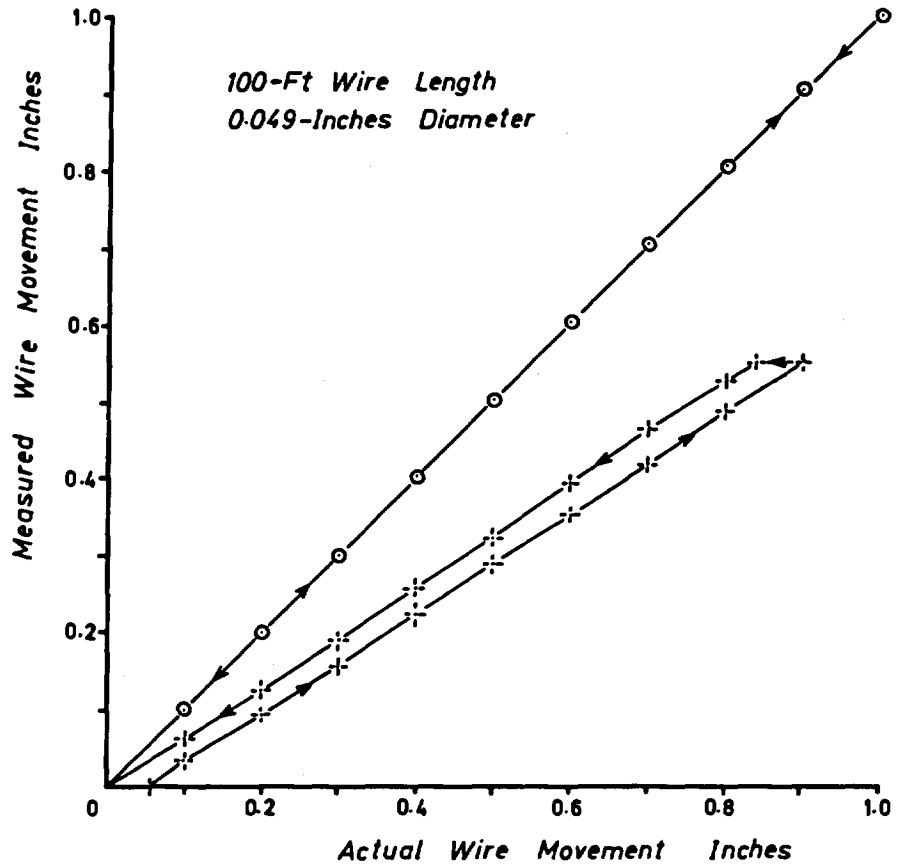
This example shows that relatively large cumulative errors can result from sag of the wire, especially if the wire is supported at intervals along the borehole. The incremental errors decrease significantly with increasing tension. Therefore, for a 100-foot unsupported wire the minimum starting tension should be about 8 lb, whereas for a 100-foot wire supported at 25-foot intervals the starting tension should be about 18 lb.

3. LABORATORY CALIBRATION OF EXTENSOMETERS

The theoretical considerations discussed in the previous sections have indicated sources of error which are potentially important and their order of magnitude for various types of extensometers and borehole configurations. It is also advisable to calibrate the extensometers in the laboratory to determine their accuracy under certain controlled conditions.

To simulate a borehole a number of 20-foot lengths of 2-inch-diameter steel pipe were connected together and a stainless-steel wire installed in the pipe. To one end of the pipe a mechanical arrangement was attached, which was capable of moving the wire over a range of 1 inch and measuring the movement to .001 inch. The extensometer was connected to the other end. The wire was moved in constant increments, away from and towards the extensometer, and the response was measured on the extensometer. Various lengths of wire could be tested by removing lengths of the steel pipe. In this way the actual and measured wire movements can be compared and the results statistically analysed to determine the accuracy. The accuracy was taken as '+2 standard errors of the estimate' from the regression line of actual against measured movement. The friction present in the extensometer can be obtained from the lag in extensometer response when reversing the direction of movement of the wire.

Figure 11 shows the calibration curves and accuracies of two types of extensometers; one which applies a constant tension; and the other where tension varies with wire movement. Wire lengths of 20 feet, 40 feet, 60 feet, 80 feet and 100 feet were used in the calibration, and the results for the 100-foot wire are shown in the graph. The calibration curve for the constant tension extensometer is linear and the measured movement is almost identical to the actual wire movement. For the variable tension extensometer the measured movement is less than the actual wire movement due to the stretch of the wire with increasing tension. Consequently, only a fraction of the wire movement is measured, which is one disadvantage of this type of instrument. Also the loading and unloading cycles are not the same due to the friction in the extensometer. The horizontal difference between the two curves (lag) is proportional to the amount of friction and wire length.



○ Constant - Tension Extensometer
 ✚ Variable - Tension Extensometer

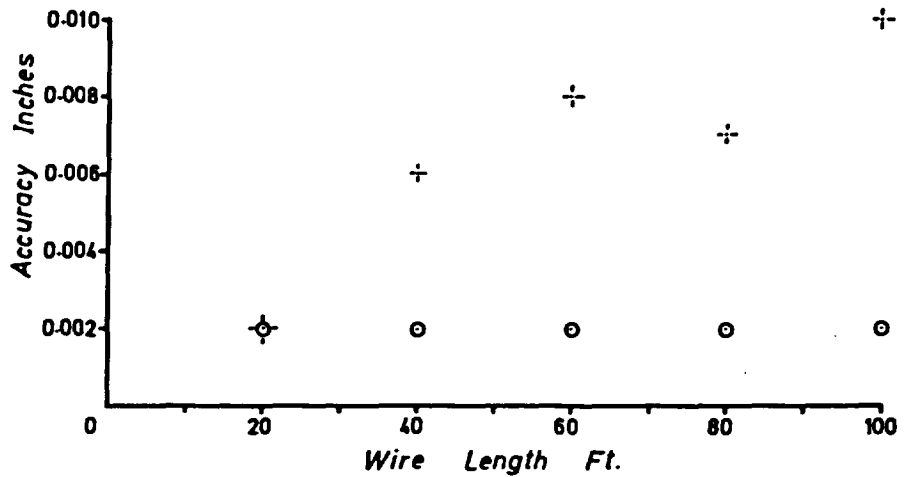


Figure 11 : Calibration and Accuracy Curves for Constant- and Variable-Tension Extensometers.

The lower graph in Figure 11 shows the accuracies of the two types of extensometers for different wire lengths. The constant-tension extensometer had a constant accuracy of $\pm .002$ inch for all wire lengths, whereas the variable-tension extensometer had an accuracy of $\pm .002$ inch at 20-foot wire length ranging to $\pm .010$ inch at 100 feet. The inherent accuracies of both extensometers (accuracy at zero wire length) is about $\pm .002$ inch. The change in accuracy of the variable-tension extensometer is due to friction in the extensometer and to the increase in the correction factor with increasing wire length.

4. PROCEDURE FOR IN-SITU READING OF EXTENSOMETERS

Accurate, repeatable readings on extensometers usually cannot be obtained just after the wires have been installed in a borehole, unless the wire has been pulled through a straightener. Otherwise, a relatively high tension is applied to each wire over a period of approximately two weeks, which tends to straighten and also dispose of the permanent stretch of the wire. This is the only procedure that can be applied to extensometers which are permanently connected to the wires. The following procedures refer to extensometers which are intermittently connected to the wires.

Before taking readings the tension on the wire should be cycled a few times between zero and a high tension. Then the tension should always be smoothly increased to the standard value, otherwise there will be hysteresis effects in the wire and frictional effects in the extensometer. Three separate readings should be taken, if they are not within acceptable limits more readings are taken and usually the highest and lowest values are neglected and an average calculated.

It is useful to take readings at two standard tensions. The difference in reading at these two tensions should be the same every time a set of readings is taken. A small change could mean that the frictional effects in the borehole have altered, while a major change could indicate that the wire is obstructed or the borehole has sheared and clamped the wires. The location where the obstruction occurs can be estimated using the equation,

$$L = \frac{x}{(T_2 - T_1)} \frac{\pi}{4} d^2 E \dots\dots\dots (\text{Eq. 18})$$

where, L = wire length, distance from collar to location of
 obstruction,
 T_1 = first tension,
 T_2 = second tension,
 x = stretch of wire for increase of tension T_1 to T_2 ,
 d = wire diameter,
 E = elastic modulus.

It should be noted that some extensometers measure the movement of the spring as well as that of the wire. The stretch of the wire is obtained by subtracting the spring movement from the measured movement.

An actual in-situ example of this technique is shown in Figure 12. Immediately after installation the plot of wire stretch against wire length is linear, which indicates a good installation with no wire obstruction. The elastic modulus can be calculated from the gradient of this line and is 23×10^6 psi. Any subsequent reading which falls below this line indicates obstruction of the wire. Whereas, readings above the line indicate that the wire was obstructed at the lower tension but became free at the higher tension, and the measurement at the higher tension is the correct one.

The second set of readings after 27 days show that the 84-foot wire was obstructed at about 67 feet, while the other wires were still free. After 68 days the 84-foot wire was obstructed at 54 feet, the 65-foot wire at 46 feet, and the 45-foot wire at 37 feet, while the 25-foot wire was still free. This obstruction was caused by fill tailings penetrating the fractured rock and blocking the borehole. Since the wires are effectively shorter than they were at installation less wire stretch takes place which would indicate an apparent expansion of the rock-mass. The technique of taking measurements at two tensions prevents erroneous interpretation of the results.

Occasionally helical springs in extensometers change their loading characteristics due to repeated loading and relaxing. These springs should be periodically recalibrated, the easiest method being to hang a weight on the spring, equal to the standard tension, and compare spring deflections.

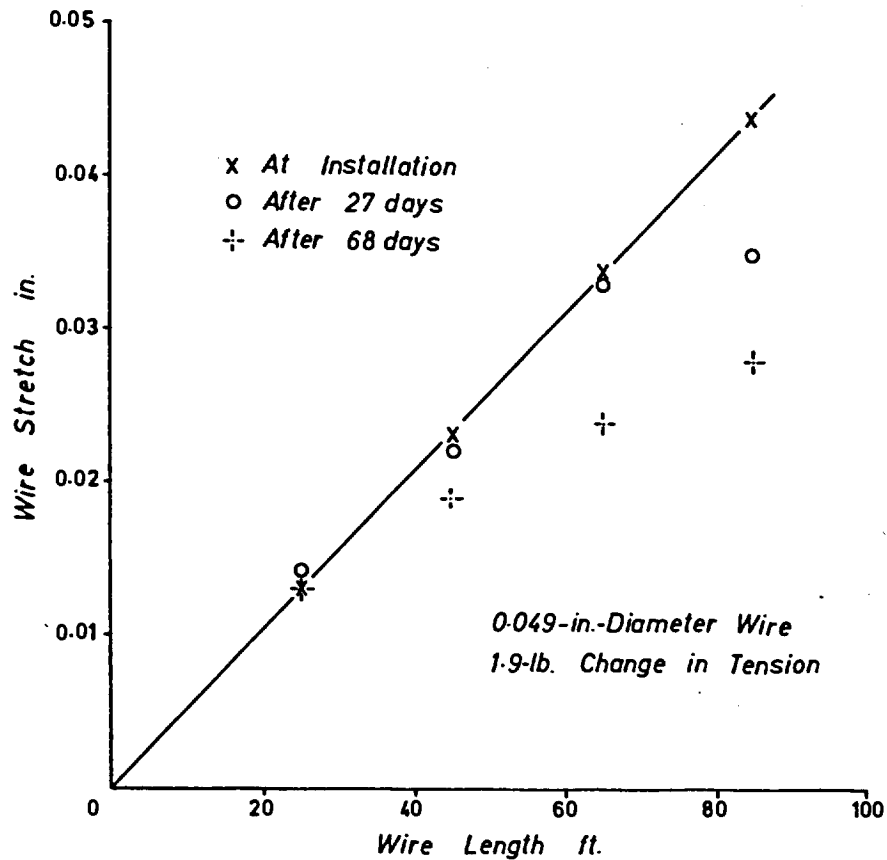


Figure 12: Example of the Interpretation of Extensometer Measurements Using Two Tensions

5. CONCLUSIONS

Rock-mass movement is generally measured with borehole extensometers. It is recommended that it be attempted to measure the movement of fractured rock to within an accuracy of .050 inch and the movement due to change in stress in continuous rock to within .010 inch, in which case the individual errors produced by various factors should be kept to within .010 inch and .002 inch respectively. The theoretical conditions discussed in this report have indicated those factors which are potentially important, and methods of reducing or eliminating their influence have been suggested.

In summary the main points are:

1. Friction in the extensometer affects the whole length of the wire and must be almost eliminated to obtain accurate measurements. This is best achieved in the design of the extensometer by having no guides for springs and by connecting the tension measuring devices immediately to the wire.
2. The error produced by friction between wire and borehole becomes significant above wire lengths of 69 feet and 154 feet for the two accuracy limits and can be reduced or eliminated by increasing the tension or number of supports for the wire.
3. Friction between the wire and anchors only becomes significant when the borehole is not straight and a component of the tension is applied to the anchors. The resultant error can be reduced to acceptable limits by using anti-friction bearings where the wires pass through the anchors.
4. Intertwining of wires can produce excessive friction and must be avoided by permanently separating the wires at each anchor and at the borehole collar.
5. Change in temperature affects both the length of the borehole and wire, and can produce large errors. Boreholes drilled from surface are affected to a depth of 25 feet below which the temperature remains almost constant. In most cases the temperature variations can be corrected for by installing a wire at 25 feet and subtracting the movement on this wire from the movements recorded on the other wires. Another method is to match the coefficients of linear expansion of the rock and wire so that both expand or contract the same amount. To obtain the movement of the borehole, including that produced by temperature, two wires with different coefficients of linear expansion are connected to each anchor.
6. The apparent elastic modulus of wire increases with increasing tension due to straightening the wire from its natural curvature. This affects only variable-tension extensometers and the effect can be substantially reduced by passing the wire through a wire straightener. Variable-tension extensometers are also affected by change in sag of the wire. Consequently, the initial tension should be high enough to reduce the error to acceptable limits.

7. Laboratory calibration of two extensometers showed that the one which applies a constant tension to the wire has the same accuracy for wire length up to 100 feet, while the variable-tension extensometer becomes less accurate with increasing wire length. The inherent accuracy of both extensometers tested (i.e. for zero wire length) was approximately $\pm .002$ inch.
8. As a general principle, constant-tension extensometers are preferable to variable-tension extensometers as they are subject to fewer sources of error.
9. The procedure for taking readings should be identical each time a set of measurements is taken. Also it is useful to read at two different tensions, since it prevents erroneous interpretation of the results and indicates the location where wire obstruction occurs.

Once the location and length of a borehole is decided together with the required accuracy, it should be possible to evaluate the errors which are likely to be important. Using the equations and graphs in this report the order of magnitude of the errors can be estimated. Then the type of extensometer, tension, wire diameter and the various methods of reducing these errors can be decided and implemented.

Abstract

The problem of pillar stability at an iron mine was investigated by measuring field and pillar stresses, pillar deformation, sonic velocity and microseismic activity. Extensometer measurements of pillar deformation provided the most useful information on the extent of load transfer and stability of the pillar. These measurements in conjunction with the observed cases of pillar cracking indicate that the structural-weakness (fault and joint) planes are the main factors affecting stability. The in situ measurements of stress and deformation are compared to those calculated from a finite-element model, in an attempt to establish an analytical method of prediction.

Introduction

In 1963 a cooperative research program was established to carry out rock mechanics studies at the MacLeod Mine of the Algoma Steel Corporation. The objective of the work was to obtain basic information on the load, and deformation characteristics of the existing mine pillars, which would assist in the solution of the problems of mining at a greater depth. It was recognized that the results of any such rock mechanics investigations would only provide supplementary information that could be added to existing mining experience.

During the last six years a number of measuring techniques have been tried. Stress, deformation, microseismic and sonic measurements have been taken at several locations in the mine. This served the dual purpose of gathering data relevant to pillar stability and of evaluating the effectiveness of the measuring techniques in this mine. In many cases the measurements were designed to be complementary; for example, pillar cracking should be picked up by the extensometer, and by microseismic and sonic measurements.

In this paper the stress, deformation, microseismic and sonic measurements are summarized and compared. The case histories of pillars which have shown visible signs of cracking have been compiled, since these pillars show the first signs of instability. An analytical model, based on the theory of elasticity and using the finite-element technique, has been constructed to investigate the stress and deformation characteristics of a pillar as mining takes place. These stresses and deformations are compared

Underground Measurements in a Steeply Dipping Orebody

D.G.F. Hedley and G. Zahary
Research Scientists, Elliot Lake Laboratory, Mining Research Centre, Mines Branch, Department of Energy, Mines and Resources, Elliot Lake, Ontario.

H.W. Soderlund
Chief Engineer, Algoma Ore Division, Algoma Steel Corporation, Wawa, Ontario.

D.F. Coates
Head, Mining Research Centre, Mines Branch, Department of Energy, Mines and Resources, Ottawa, Ontario.

to those measured in situ. Using all this information the critical parameters controlling the load applied to, and support offered by, the pillars can be more fully understood.

Description of the Mine

Algoma Ore Division of Algoma Steel Corporation operates both an underground mine and an open pit at Wawa, Ont., on the southwestern end of the Michipicoten iron range. The combined production from both operations is about 3,250,000 gross tons of siderite ore per year.

Geology

The Michipicoten iron range, which contains all the presently known orebodies, lies within a complex assemblage of Precambrian volcanic and sedimentary rocks. The siderite-pyrite orebody is bounded on the hangingwall by a volcanic series and on the footwall by a banded iron formation.

Structurally the orebody lies on the south limb of an east-to-west-trending syncline which has slightly overturned toward the north and plunges 40 to 60 degrees eastward. Thrust faults dipping 15 to 30 degrees south have

displaced the ore zones northward and up. Two major thrust zones, separated vertically by 500 to 700 feet, are known to exist. These thrust zones considerably influence stope and pillar dimensions. The orebody dips generally at 70 to 80 degrees south but the flat thrust zones produce an overall dip of about 65 degrees.

In the central part of the orebody two steeply dipping diabase dikes intrude along major fault planes striking northwesterly, as shown on the plan of the M1 level, Figure 1. This major structural feature offsets the west and east section of the mine by about 300 to 400 feet. The mining zone terminates to the east at another diabase dike where major faulting displaces the iron formation.

Method of Mining

The George W. MacLeod mine has been developed along a strike length of one mile to a depth of 2,000 feet. The orebody is mined by a sub-level, longhole, open stope-and-pillar method. The main levels are driven on 300-ft vertical intervals and sub-levels on 75-ft centres.

Stopes are 60 to 75 ft along strike and usually 230 ft high. Pillars are 75 to 80 ft along strike and take the form of an inverted letter 'L'. The crown pillar overlies the adjacent stope and extends to the level above. The stope and pillar dimensions in some sections of the orebody differ from the above because of geological structures, intrusives and grade considerations.

A stope is normally blasted, over a period of several months, in rings 5 ft apart. The pillars are taken out in two large blasts, first a 15-ft slash then the remainder of the pillar.

The dimensions of the MacLeod orebody and the overlying mined-out Helen orebody are such that large openings are created. The comparatively low grade of the ore precludes the use of back-filling and consequently the mining sequence is planned to take advantage of natural caving of the hangingwall. At present, in the west section of the MacLeod mine, the ore has been removed over a strike length of about 800 ft to a depth of 1,000 ft, as shown in the longitudinal section, Figure 1. Caving of the hangingwall and ore lost through dilution has

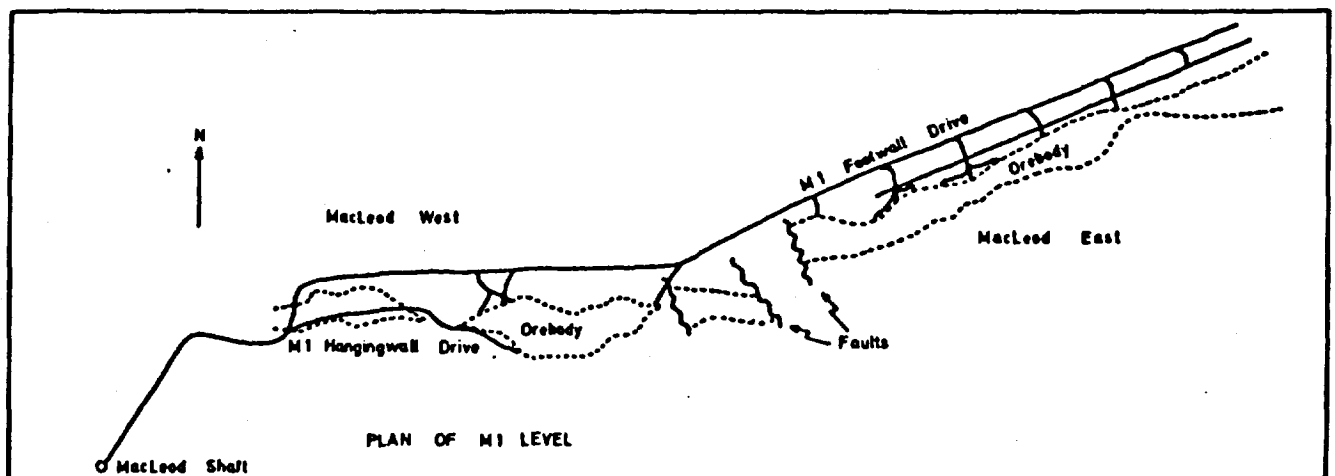
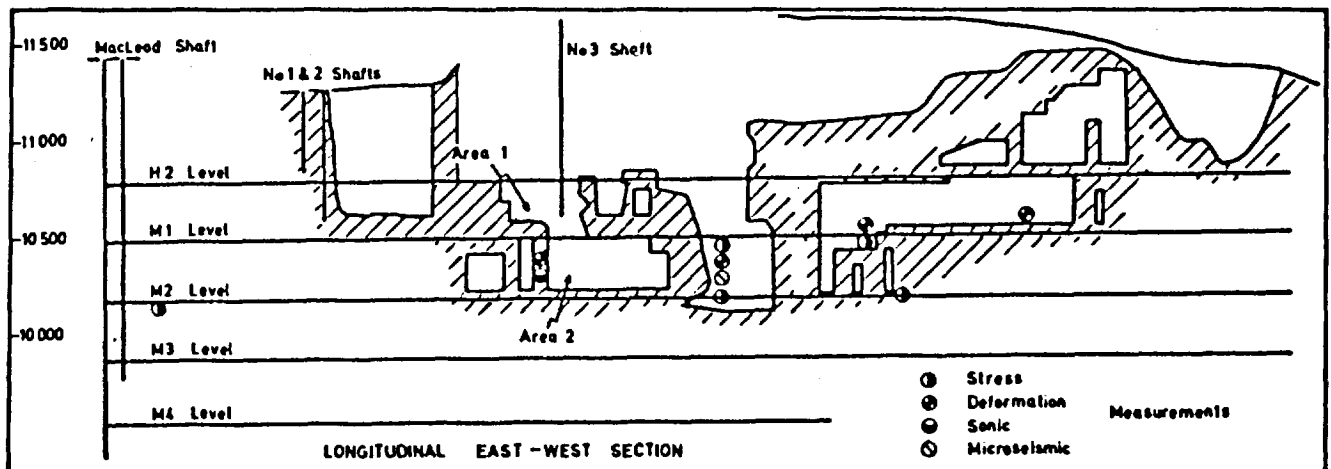


FIGURE 1 – Section and plan of the MacLeod mine showing location of instrumentation sites

provided a cover of about 200 feet of broken rock over the active workings.

It was expected in the early planning stages that the hangingwall would slough readily, but experience now indicates that the hangingwall will stand up vertically over the spans mined to date. Consequently, it is now the intention to leave four semi-permanent pillars, two in each of the east and west sections of the mine. These pillars will be approximately 225 feet wide at about 800-foot centres and extend from the top to the bottom mining level.

The overall mining sequence is planned to retreat east and west from the centre of the orebody, with the east and west mining faces on any level being 500 ft ahead of the mining faces on the level immediately below. Consequently, from the point of view of ground control there are no open stopes below active mining operations.

Measuring Techniques

The longitudinal section of the mine, Figure 1, shows the locations at which measurements of stress, pillar deformation, sonic velocity and microseismic activity were taken. The general methods of measurements are outlined in the following sections.

Stress

An overlying technique was used to determine the stresses acting on the orebody; the principle being that the rock, when the stresses are removed by overcoring, relaxes and the magnitude of the relaxation is proportional to the stresses originally acting on the rock. By measuring relaxation in three orientations in a borehole and knowing the elastic properties of the rock, the magnitudes and directions of the principal stresses can be calculated for the plane perpendicular to the axis of the borehole. This method of measurement gives the stress values at the time of overcoring but does not give directly the increase in stress resulting from mining. The USBM deformation meter was used as the sensing device and the change in diameter of an EX borehole was measured when overcoring with a 6-in. dia. bit.

Extensometer

Borehole extensometers measure the relative movement between the collar and a point in the borehole. Usually the rock movement is the result of mining and it is measured over a period of time.

Both bolt and multi-wire extensometers have been used at the mine. The bolt extensometer consists of a rock-bolt shell and rod anchored in a borehole. The end of the rod protrudes through a sleeve at the borehole collar, and a dial gauge measures the movement between rod and sleeve. A separate borehole is required for each bolt. With the wire extensometer, as many as four wires can be installed in one borehole. The longer wires pass through holes drilled in the anchors. The extensometer is intermittently connected at the borehole collar and measures the relative movement between wire and borehole.

Sonic

This technique involves a measure of the transit time of a compressional sonic wave between a transmitter and a receiver probe anchored in two boreholes. A signal is generated by tapping a pipe connected to the transmitter, and the transit time is measured by means of an oscilloscope. The velocity of sound through rock is basically dependent on the elastic properties of the rock; however, the velocity can be considerably altered by the structural-weakness planes in the rock mass.

Microseismic

The Seismitron is an instrument for detecting sub-audible noises in rock. Used in its simplest form a geophone is lowered into a short borehole and the number of amplified sounds, as heard on earphones, is recorded over a certain time interval. In an area where the background level of noise is constant, any increase in the number of sounds is an indication of increasing stress and possible instability.

Results of the Measurements

Stress

A program of measurements was undertaken to determine the field stresses acting in the orebody and the pillar stresses. It was expected that stress values, representing an order of magnitude, could be obtained from a few observations. This involved certain assumptions including a homogeneous stress field around the orebody and elastic behaviour of the rock mass.

The locations of the stress measurements are shown on the longitudinal section, Figure 1. Measurements were made at different locations in the borehole to a depth of 20 ft to define

the stress concentration, and results from the bottom part of the hole were used. The stresses of greatest interest are those acting parallel and perpendicular to the axis of the pillars and consequently parallel and perpendicular to strike of the orebody. For practical purposes, all holes were horizontal and measurements were made in a vertical plane.

Pre-mining field stress parallel to strike was measured in a borehole drilled in hangingwall tuff. The site was on the M2 level near the shaft, 1,500 ft from the nearest mining and some 1,300 ft below surface. A maximum stress of 6,500 psi dipping 20 degrees to the east was obtained. A similar measurement was made, on the same level, 4,000 ft to the east in footwall iron formation. Mining had been completed 300 ft above and 700 ft to the west of the site. An average of 5,000 psi between 10 and 20 ft in the hole was obtained for the maximum stress which dipped 10 to 20 degrees to the east.

Another borehole was drilled in the footwall iron formation to measure stress perpendicular to strike of the orebody. The maximum stress was of the order of 4,000 psi acting perpendicular to the walls.

Pillar stresses of the order of 2,500 to 3,000 psi perpendicular to the hanging wall and footwall were measured in pillars 242 and 251. The mining geometry for both sites was similar in that an opening of about 200 ft existed on one side of the pillar and a 60 ft open stope on the other. In addition, a borehole was drilled on the M2 level directly below pillar 242. In this case a maximum stress of 5,000 psi was measured perpendicular to the hanging wall and footwall.

The vertical field stresses were found to vary between 1,700 psi and 2,900 psi. The gravitational load is of the order of 1,400 psi at all locations.

The data indicates that vertical stresses can be double the gravitational load; horizontal stresses are greater than the vertical; and the stress parallel to strike is greater than the perpendicular stress. Hence, if the data is accepted at face value, previous tectonic history rather than depth provides a more logical explanation for the observations.

On the other hand, the measurements obtained here are not conclusive. Departures from the original assumptions do occur. A high stress concentration around the mine opening and an area of uniform stress beyond was not always

obtained. Planes of weakness in common mine rocks are considered to be a major contributing factor. Weakness planes on the scale at which the instrumentation operates produce large fluctuations in results.

On the basis of this work the concept of an average stress field around the orebody is retained. The principal stress acting parallel to strike is of the order of 5,000 psi, the intermediate stress acting perpendicular to strike, 2,500 to 5,000 psi, and the minor principal stress acting vertically, 1,500 to 3,000 psi. Other sources of information must be used to establish whether the measurements are adequate. Discontinuities in rock appear to be a significant factor in producing fluctuating results. This implies that measurements should be made with much closer geological correlation.

Extensometer

In general, the purpose of the borehole extensometers was to measure the deformation of a pillar as mining takes place in the vicinity. Of specific interest were the nature and order of magnitude of the movement, the locations in the pillar where the movement occurred, and the distance over which mining affected the pillar. The locations of the extensometer sites in pillars 242, 251, 163 and 228 are shown on the longitudinal section, Figure 1, and the enlarged individual sections and plans for each site in Figure 2.

The measurements taken in pillar 163 gave a comprehensive picture of pillar deformation. Extensometers were installed from a central crosscut and measured at intervals along the three axes of the pillar. Measurements started at the beginning of mining and ended with the pillar being blasted out. The graph of total deformation of pillar 163 is shown in Figure 3. These three curves represent the movement in each direction of the end measuring points relative to each other. A record of the time over which the stopes were mined and pillars removed is given below the time axis of the graph.

It is possible to relate, qualitatively, pillar deformation to mining activity from this graph. Between hanging wall and footwall, mining of the adjacent stopes 162 and 164, and the 163 pillar slash, produced appreciable deformation (compression), whereas mining stope 166 and pillar blasts 157, 159, 161 and 165 had no significant effect. The individual measurements

along this axis showed that the major movement took place at the centre of the pillar and there was little movement at the hanging wall and footwall. This indicates a stress parallel to strike considerably higher than that perpendicular to strike.

The expansion measured in the vertical direction increased slowly while mining stope 164, 165 pillar blast, and 163 pillar slash. The individual measurements showed that the expansion was almost totally confined by 15 ft above and 30 ft below the crosscut, and the movement between roof and floor of the crosscut was also expansion. These observations could result from a compressive stress acting between hanging wall and footwall, higher than the vertical stress. Also the open stopes, above pillar 163, will have partially diverted the gravitational load to the hanging wall and footwall.

Relatively large expansion was measured between the east and west sides of the pillar during the mining of stopes 162 and 164. The first pillar blasts 157, 159 and 161 had little effect, but 165 pillar blast and 163 pillar slash as well as mining stope 166 resulted in considerable expansion. It would seem that expansion on the east and west sides of the pillar during and after the mining of stope 166 was mainly due to the disturbance caused by blasting rather than the transfer of load, since no significant movement was measured between hanging wall and footwall during the mining of stope 166 and the 165 pillar blast.

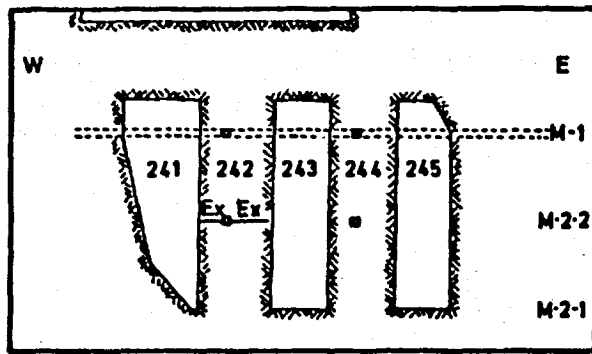
The profiles of lateral expansion across pillar 163 in the east-west direction are shown in Figure 4. Most of the expansion was confined to the outside of 14 ft of the west side of the pillar during the mining of the adjacent stope 162 (curve 1). The largest deformation gradient, indicating possible cracking, was between 9 and 14 ft from the pillar edge. This pattern of movement was repeated during the initial mining in stope 164 and the 161 pillar blast (curve 2). On the completion of mining stopes 164 and 166 and the 165 pillar blast, the expansion of the 14 ft at the west side of the pillar increased appreciably (curve 3) indicating definite cracking within this zone. Also expansion occurred on the east side of the pillar with the maximum deformation gradient being within 10 ft of the pillar edge. During all this mining activity the central 50 ft of the pillar remained relatively undisturbed. However, there was a

general overall expansion when a 15-ft slash was taken off the east side of pillar 163.

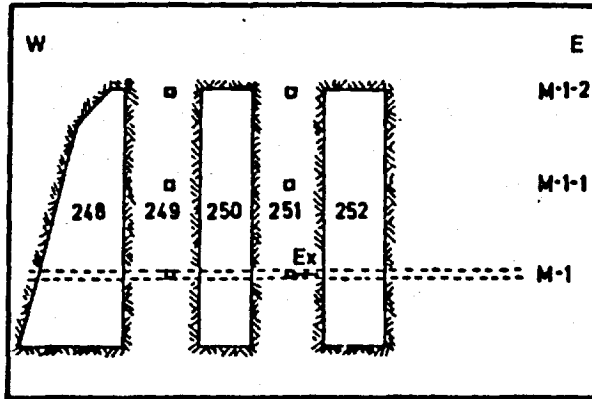
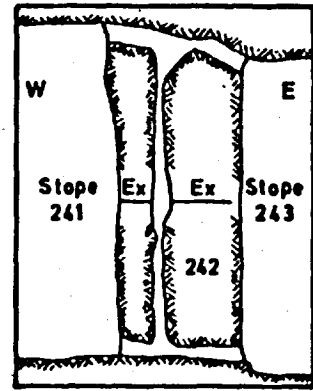
Extensometer bolts were installed in the west side of pillar 228 (Figure 2) after stope 229 on the east side was near completion. Beyond pillar 230 the opening span was 400 ft to pillar 236. Above pillar 228 the stopes and pillars had been mining out. The extensometers measured the lateral expansion of the pillar as stope 227 was mined and pillars 230 and 236 blasted. Curves 4, 5 and 6 in Figure 4 show the profile across the west side of the pillar. Curve 4 is after the 230 and 236 pillar blasts and curve 5 after stope 227 had been partially mined. These two curves indicate that the major expansion was taking place within 5 ft of the centre crosscut with little movement in the rest of the pillar. At this time a diagonal crack was observed running the general direction northwest to southeast which intersected the 5-ft extensometer bolt. On completion of mining in stope 227 (curve 6) there was an overall expansion of the west side of the pillar with the edge moving about 3/4 in., indicating intensive cracking of the pillar.

Measurements of lateral pillar expansion were taken in both the east and west directions in pillar 242, as pillar 244 and stope 241 were mined (Figure 2). The pattern of movement was similar to that obtained in pillar 163, although the magnitude of the expansion was much less. Extensometers installed in the east side of pillar 251 recorded very little expansion during the mining of stope 252 (Figure 2).

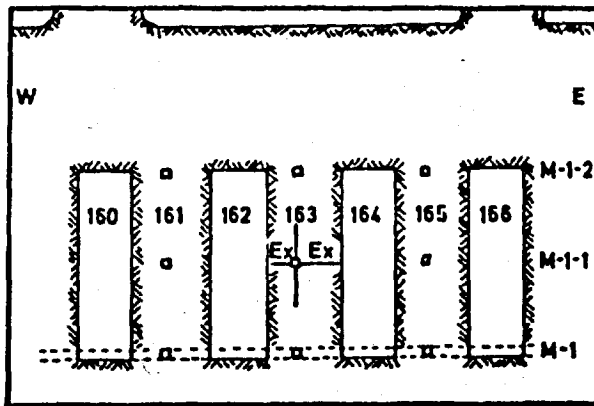
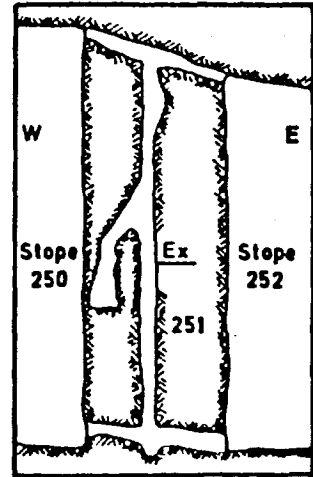
The measurements of lateral pillar expansion show that the movement is closely related to nearby mining and takes place along pre-existing joint and fault planes. These geological weakness planes are probably the determining factor concerning pillar sloughing and instability. A structural geological study has been undertaken in pillars 167 and 228 representing the east and west sections of the mine (G. Herget, private communication). It was found that in the east section the joint frequency was much greater than in the west. In addition, the two major joint sets in the east were oriented parallel to the pillar sides and perpendicular to the dip of the orebody, whereas in the west the two major sets of joint and fault planes were nearly vertical and extended diagonally across the pillar. Consequently, the pattern of pillar deformation is likely to be different in the east and west sections. In the east, as exemplified by



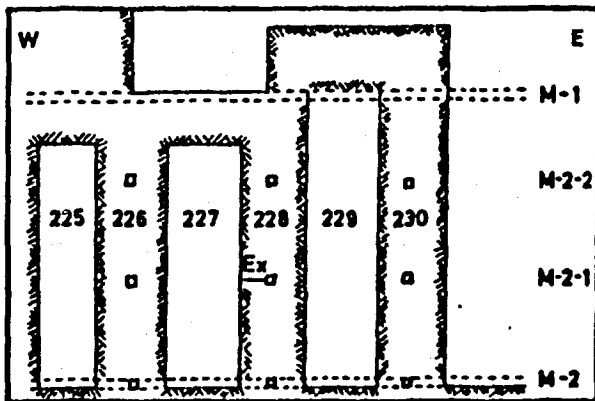
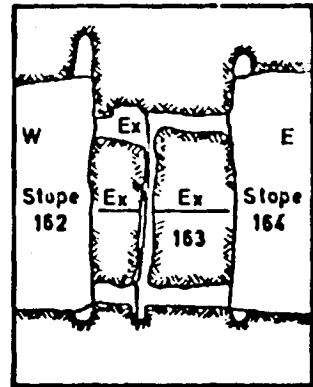
East - West
Section and
Plan of
Pillar 242



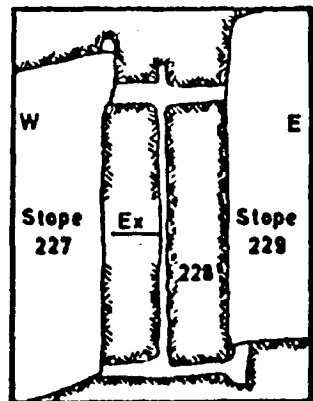
East - West
Section and
Plan of
Pillar 251



East - West
Section and
Plan of
Pillar 163



East - West
Section and
Plan of
Pillar 228



SECTIONS

PLANS

FIGURE 2 - Section and plan of extensometer measuring sites

pillar 163, lateral expansion is concentrated at the sides of the pillar and the rock expands toward the open stopes. In the west, as exemplified by pillar 228, shearing movement takes place along a diagonal fault or joint which intersects the centre of the pillar.

Sonic

Sonic velocities were measured in the 228 pillar near the extensometer site. It was expected that cracks would develop in the pillar as load and confinement were altered by mining. Sonic velocity decreases in fractured rock and the measurements over a period of time could indicate developing pillar instability. Consequently, measurements were repeated at three- to four-month intervals at each location in the pillar.

Two rings of probe holes were drilled 15 ft on either side of the bolt extensometer. Each ring consisted of 6 ft vertical, 25 ft horizontal and two intermediate inclined holes. This configuration provides a number of transmission paths of which 16 were chosen; most of these were parallel to the three axes of the pillar.

During the period of measurement, the 230 and 236 pillars were removed and the 227 stope advanced. The extensometer measurements showed (Figure 4) that a diagonal crack developed which intersected the 5-ft bolt and also the transmission path of the sonic pulse. However, the measurements of sonic velocity varied by less than 10% during this period. Eventually, one set of holes was cut-off by the diagonal crack.

Transmission time is measured to within 5% by the oscilloscope. The field work was done in an active mining area where the background noise level was high and it was difficult to obtain accurate and consistent measurements. Consequently, a difference in sonic velocity of less than 10% is interpreted as not being significant.

The average velocities measured parallel to the pillar axes are given in Table 1. Previous work in the laboratory established that the longitudinal-wave velocity in siderite was of the order of 18,500 – 20,000 ft/sec. The measurements obtained in the present series of tests are slightly higher than those obtained in intact rock (no discontinuity) in the laboratory.

Although the sonic apparatus is designed to measure longitudinal-wave velocity, transit times are quite often measured, which seem to give reasonable values for the shear-wave velocity. These values are also given in Table 1.

Using the average longitudinal- and shear-wave velocities, Poisson's ratio was calculated to be 0.23. The elastic modulus of the rock, which is related to the longitudinal-wave velocity and Poisson's ratio, was calculated to be 17×10^6 psi. The elastic modulus obtained for siderite from compression tests on small samples in the laboratory, ranges between 13 and 21×10^6 psi, which is the same order of magnitude as that obtained from the sonic tests.

In summary, the sonic measurements indicate no general deterioration in the pillar rock. The one isolated crack which developed did not result in any significant change in sonic velocity. The velocities measured along the three pillar axes are consistent and give reasonable values for the elastic constants of siderite.

Microseismic

Four sites were established in pillar 242 to monitor microseismic activity. These consisted of a 5-ft hole drilled into the pillar wall. Three sites were located on the same level, one at the centre of the pillar and the others in two outside corners. A fourth site was located at the base of the pillar some 100 ft below.

Blasting of pillar 244 immediately to the east resulted in a 50% increase in the number of noises. This increased activity continued for about three weeks in the pillar corner facing the

TABLE 1
Results of Sonic Tests

	Along Strike	Normal to Strike	Vertical	Average
Path length, feet	15	30	10	
Longitudinal-wave velocity, ft/sec	20,865	19,974	20,218	20,350
No. of readings	7	16	6	
Shear-wave velocity, ft/sec	11,151	12,352	12,630	12,040
No. of readings	6	4	1	

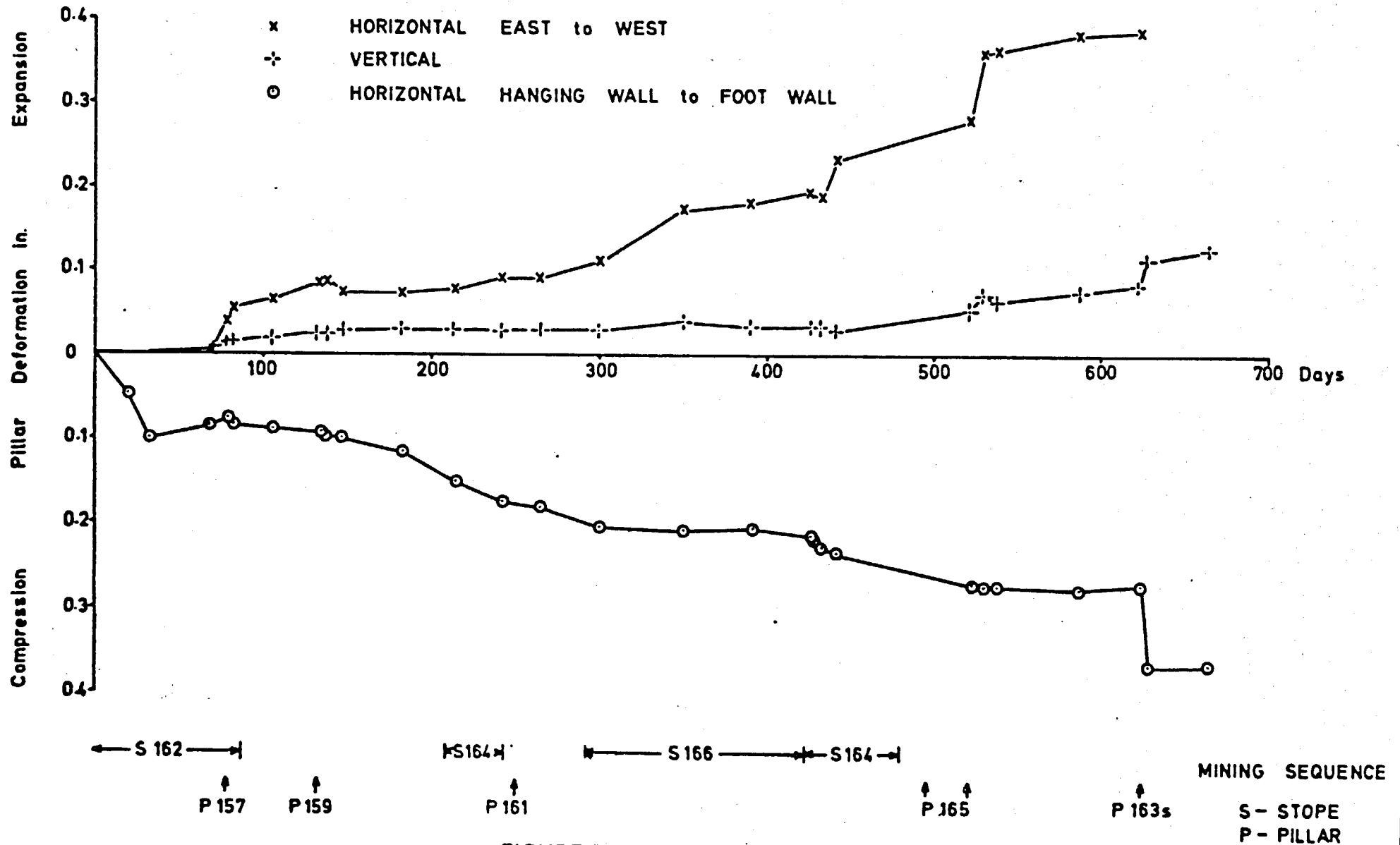


FIGURE 3 - Deformation of pillar 163.

S - STOPE
P - PILLAR

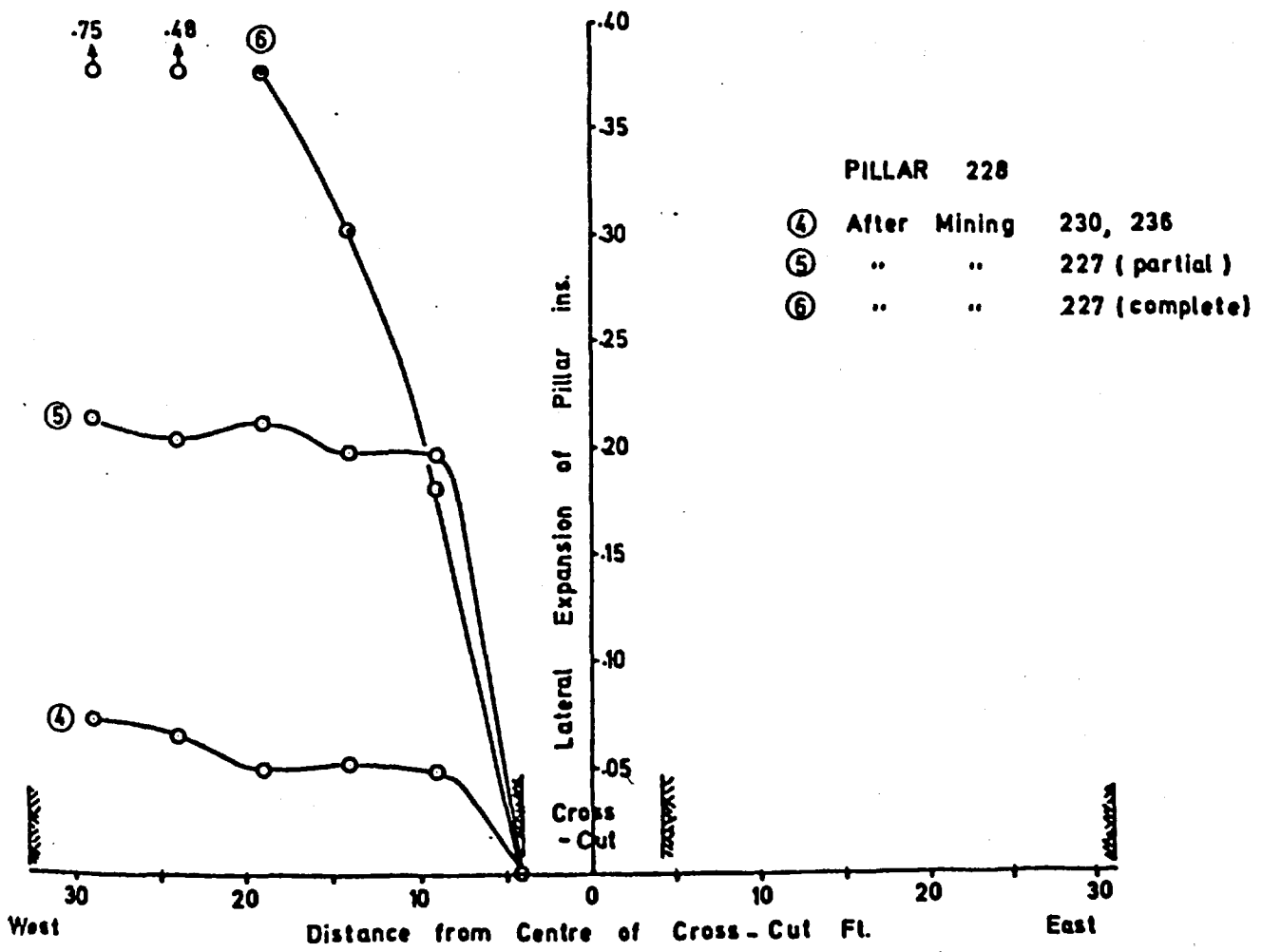
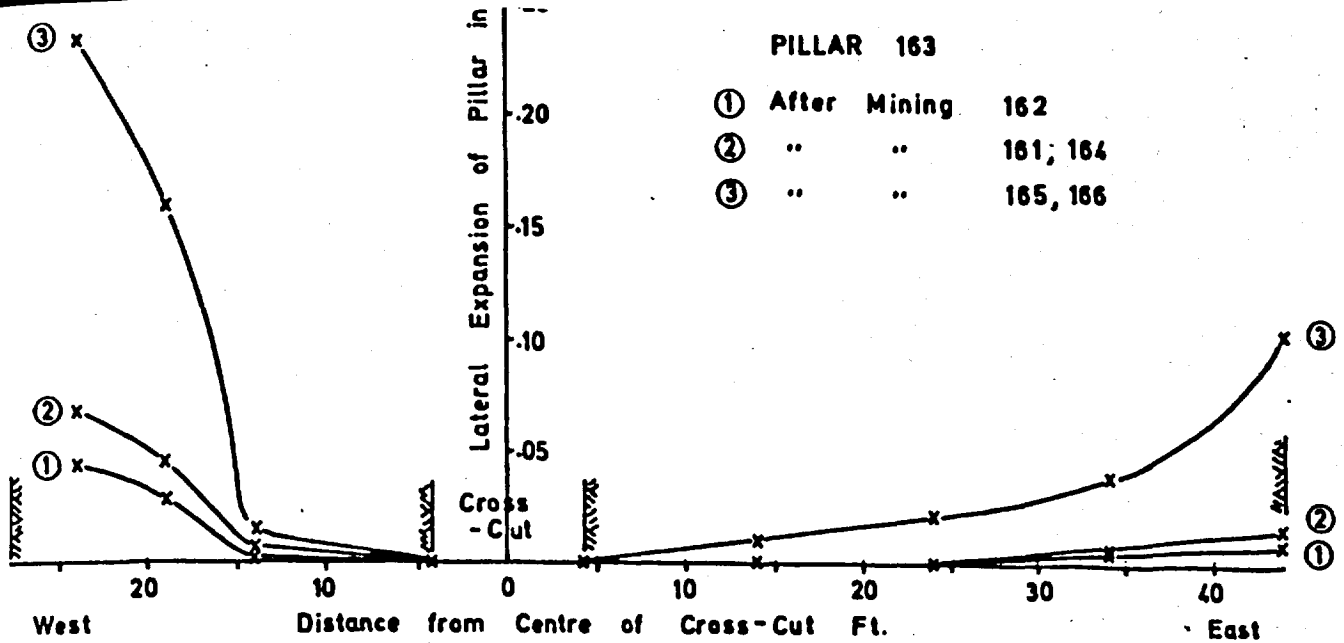


FIGURE 4 - Profiles of lateral expansion, pillars 163 and 228

blast and for one to three weeks at the other sites. Lower noise counts were obtained at the base of the pillar than at mid-height. Subsequently the noise counts declined until the pillar was removed.

Measurements were made in an upper level to monitor stability of an unsupported section of the hanging wall. Between 50 and 100 noises were recorded in different 10-minute intervals. The noise level remained constant and failure in the wall was not observed.

Another series of observations in a crown pillar at the bottom of the mined-out area produced counts of the order of 250 noises/10-minute interval following a 9,000-ton pillar slash. The noise level declined more-or-less linearly in the following two months until the pillar was removed.

The technique was applied here to monitor the stability over large distances, say 100 ft or more. Although the measurements are easily obtained they are difficult to interpret, where the problem is on such a large scale. One of the problems is that the measurement is largely subjective. The operator must choose between the various tones and loudness of the noises without knowing the origin and, hence, significance of any particular noise.

Theoretical Pillar Stresses and Deformations

At present, any theoretical prediction of pillar stresses or deformations can only be made with a two-dimensional analysis. The geometry of the MacLeod mine does not lend itself well to a two-dimensional idealization, which essentially requires that the variations in geometry occur in one plane, with the configuration in the third dimension being essentially constant. In spite of the difficulty, analyses have been made that provide some insight into the reactions, due to adjacent mining, that can be expected in the pillars.

A section, approximately horizontal, has been taken through the first sub-level of a typical pillar as shown in Figure 5. By making a two-dimensional analysis in this plane the implicit assumption is that the geometry is continuous in the third dimension. However, it is only continuous for 100 ft above and below this section, which is of the same order of magnitude as the dimensions of the stopes and pillars. Consequently, load will be diverted above and below the stopes as well as laterally to the pillars. The mining of the crown pillars

above the stopes will result in additional transfer of the stresses to the pillars and below the stopes, it being impossible to transfer through the mined-out upper stopes.

The stopes and pillars as shown in Figure 5 were part of a larger model loaded in the directions normal (N - S) and parallel (E - W) to strike. This model was divided up into a series of finite elements, and the effects of mining adjacent stopes and pillars on a remaining pillar were analyzed using the finite-element technique (Wilson). The sequence of mining in the model was: stope No. 1, stope No. 2, stope No. 3, pillar No. 4, stope No. 5, pillar No. 6, and pillar slash No. 7. Based substantially on tests on the rock substance, it was assumed that the modulus of deformation of the rockmass was uniform and equal to 10×10^6 psi with a Poisson's ratio of 0.2. It was further assumed that the field stress normal to strike, S_o , was 2,500 psi and the field stress parallel to strike, S_t , was 5,000 psi.

The overall deflection of the walls and pillars due to the mining of stopes and pillars No. 1 to No. 6 is superimposed, to an exaggerated scale, on the mine section in Figure 5. The barrelling of the pillar and the bowing-in of the walls are to be expected. However, the absolute movement of the pillar laterally is less likely to be anticipated and must result in a certain amount of working and loosening of the pillar. This lateral movement is even greater during the first stages of mining.

Figure 6(a) shows the movement in the pillar along section B - B relative to the pillar centre at the various stages of excavation. This graph would be comparable to that obtained from a borehole extensometer with the collar at the pillar centre and anchor points at 20, 40 and 60 ft toward the hangingwall or footwall. These curves are similar to that shown in Figure 3, showing that the deformation from hanging wall to footwall in pillar 163 increases with progressive mining of adjacent stopes and pillars. The mining of stopes No. 3 and No. 5 have a very large effect (Figure 6(a)) on the deformation of the pillar, as does the excavation of the adjacent pillar No. 6. The movement per unit length (strain), represented by the spacing between the curves, is greatest at the centre (0 - 20 ft) and decreases toward the walls (40 - 60 ft).

Figure 6(b) shows the profiles of pillar stress in the direction normal to the walls along

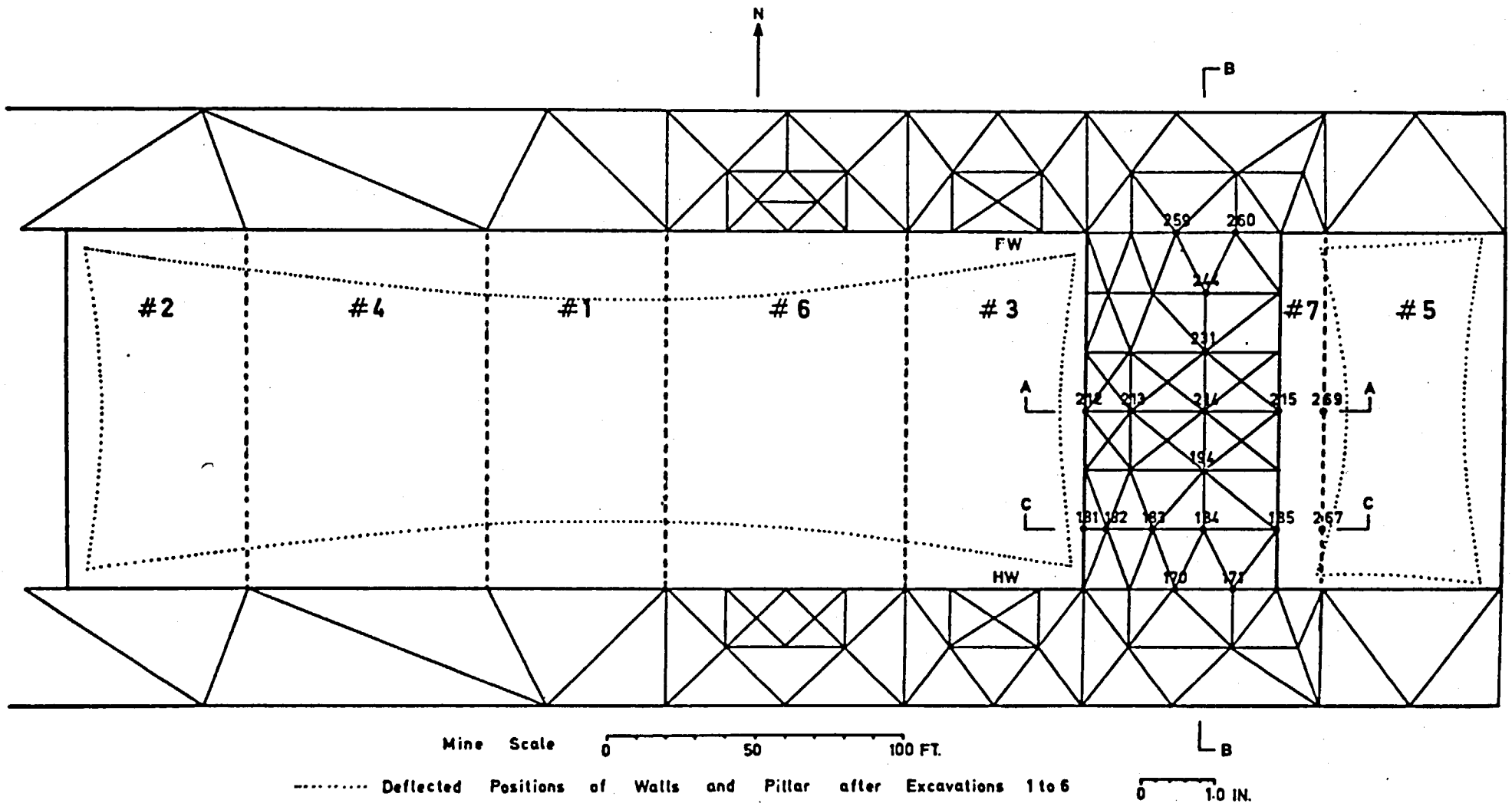


FIGURE 5 - Finite-element Model

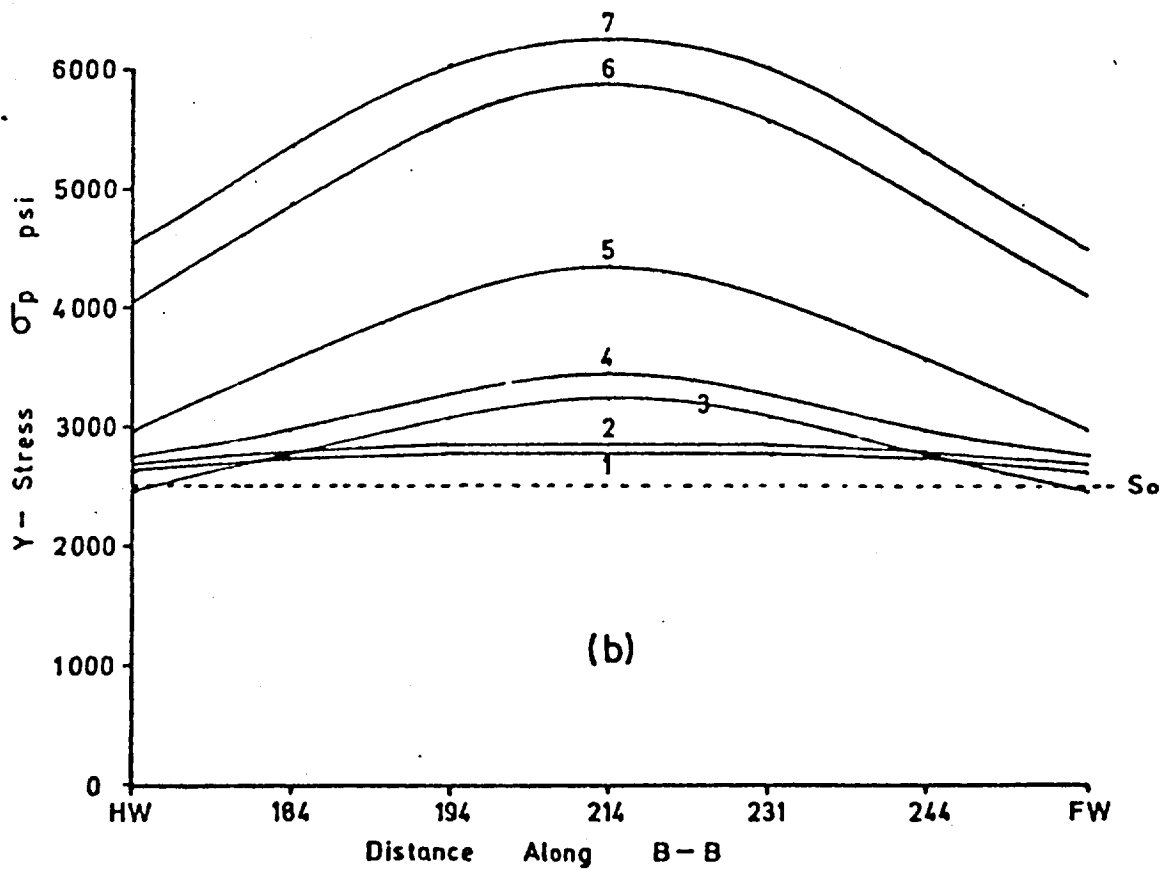
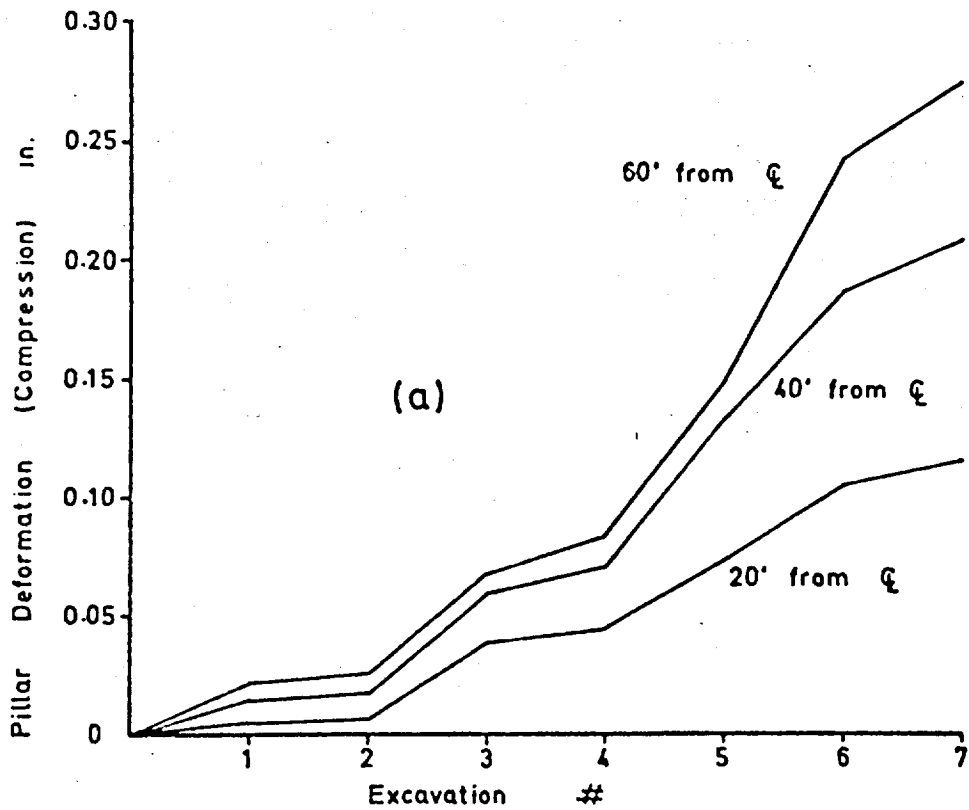


FIGURE 6 — Pillar deformation and stress profiles along section B-B, $S_0 = 2,500$ psi.

the section B — B. The profiles show the increase in stress resulting from successive excavations and the increasing difference in stress between the central portion of the pillar and the zones adjacent to the walls. This stress difference as well as the increase in transverse stress toward the walls accounts for the decrease in pillar deformation near the hanging-wall and footwall.

Figure 7(a) shows the displacements across the pillar at section A — A. It can be seen that excavations No. 1 and No. 2 result in a general movement of the pillar to the west. Excavation No. 3 causes an even greater movement to the west as well as a large increase in the expansion between the two sides of the pillar. Excavation No. 4 has little effect. Excavation No. 5 results in a movement back toward the east as well as increased expansion; excavations No. 6 and No. 7 have similar effects.

Figure 7(b) is a re-plot of the lateral pillar expansion along section A — A, comparable to a borehole extensometer with the collar at the pillar centre and anchor points at 25 and 40 ft toward the east and west sides of the pillar. It can be seen that mining stopes No. 3 and No. 5 on either side of the pillar produced most of the expansion.

Figures 7(c) and 7(d) show the profiles of axial pillar stress across the pillar at sections A — A and C — C. The stress pattern is different at the two sections; at A — A the stress is highest at the centre and decreases toward the pillar sides, whereas at C — C it is completely the opposite. It is interesting to see the conspicuous decrease in pillar stress at the west side of the pillar, section A — A, resulting from mining the adjacent stope No. 3. Then with the mining of stope No. 5 on the other side of the pillar these low stresses are increased to give a symmetrical distribution across the pillar. Curiously, the mining of pillar No. 6 results in a relatively large increase in stress on the west side of the pillar contrary to the results of mining stope No. 3. The transverse stress along section A — A was found to be reduced to zero after the excavation of the adjacent stopes No. 3 and No. 5. Along section C — C the restraint coming from the walls was found to be sufficient to preserve a considerable portion of the original stress parallel to strike in the central part of the pillar.

Table 2 shows comparative figures obtained from field measurements of the longitudinal

compression and lateral expansion. The measurements are by borehole extensometers (BIIE) and the predictions by the finite-element analysis (FE). The predicted figures are obtained from the above analysis using the incremental deformations resulting from the mining of whichever excavations No. 1 to No. 7 are equivalent to the actual block that was excavated. Furthermore, the results from the finite-element analysis are adjusted to correspond to the actual measuring lengths in the pillar.

The measured and predicted results for pillar 163 given in Table 2 are separated into two groups: the total measuring lengths (106 ft N — S, and 68 ft E — W) and over the central portion of the pillar (45 ft N — S and 38 ft E — W) which is relatively unaffected by the constraint of the walls and the zones of cracking at the sides of the pillar.

For the overall movement, the mining of stope 162, pillar 159 and the first stage of stope 164 produced poor agreement for the lateral east-west expansion but good agreement for the longitudinal north-south compression. The mining of blocks 161, 166, second stage of 164, 165 and 163 pillar slash caused the differences between measured and predicted movements to converge in the east-west direction and diverge in the north-south direction.

The measurements in the east-west direction started a month after those in the north-south direction during the mining of stope 162. Consequently, part of the east-west expansion was not measured. If the comparison is made for the mining of block 159 onward then the measured expansion is always greater than the predicted expansion, i.e. after mining pillar 165 the measured movement is 0.30 in. and the predicted movement is 0.22 in. This means that the measured movements might include non-elastic deformation, possibly due to the opening of cracks and joints as deduced from the profiles of lateral expansion shown in Figure 4.

The movements measured in the central portion of the pillar show poor agreement in the east-west direction. After mining of stope 162 no significant east-west expansion was measured until the second stage of mining in stope 164, and there was a large expansion with the 163 pillar slash which probably caused cracking throughout the pillar. The predicted movements show a general increase in expansion for

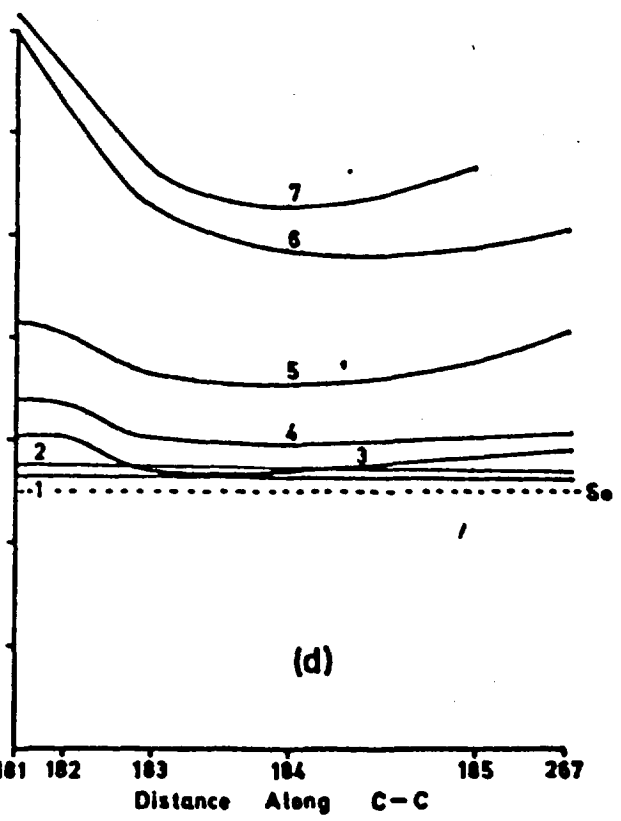
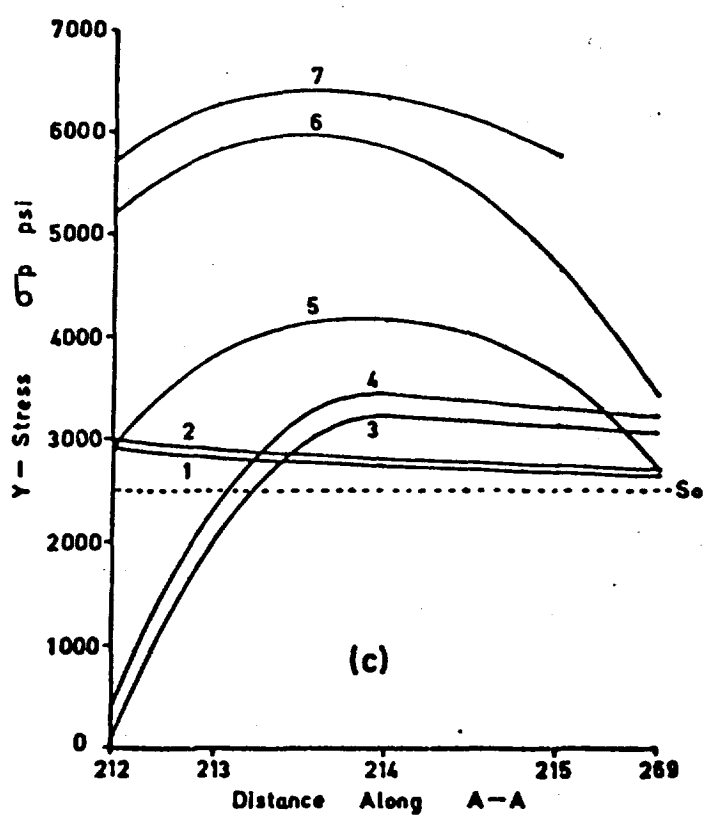
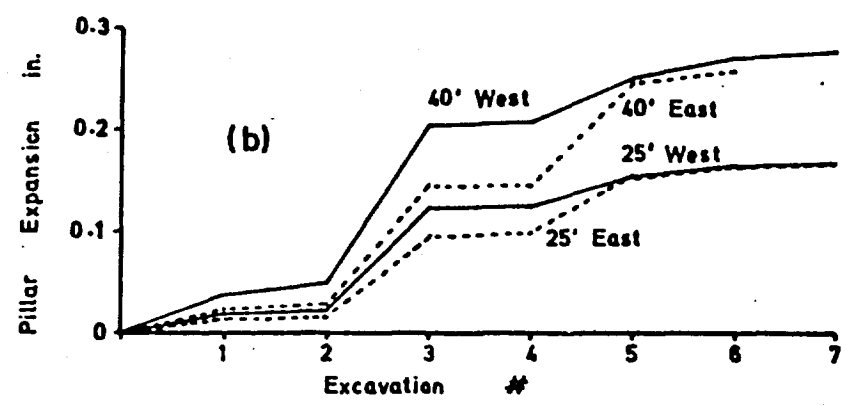
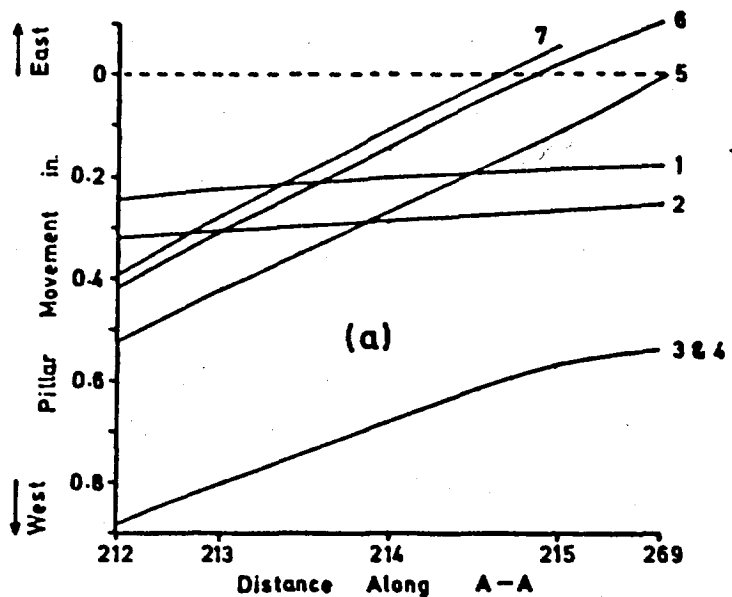


FIGURE 7 – Pillar movement, deformation and stress profiles along Sections A–A and C–C, $S_0 = 2,500$ psi.

TABLE 2
Longitudinal Compression and Lateral Expansion of Pillars
Due to Adjacent Mining of Blocks at the MacLeod Mine,
Measurements vs Predictions

Pillar Site	Block Excavated	Disp'ts E - W		Disp'ts N - S		Measuring Lengths
		BHE** in.	FE*** in.	BHE** in.	FE*** in.	
163	162	0.06	0.21	0.09	0.08	N - S 106 ft E - W 68 ft
	159	0.08	0.21	0.10	0.11	
	164*	0.10	0.28	0.17	0.17	
	161	0.10	0.30	0.18	0.33	
	166	0.20	0.34	0.22	0.37	
	164*	0.28	0.41	0.27	0.43	
	165	0.36	0.43	0.27	0.59	
	163			0.37	0.65	
163	162	0.03	0.14	0.11	0.04	N - S 45 ft E - W 38 ft Central portion of pillar
	159	0.02	0.14	0.12	0.06	
	164*	0.02	0.17	0.16	0.09	
	161	0.02	0.19	0.17	0.16	
	166	0.02	0.22	0.19	0.18	
	164*	0.05	0.25	0.22	0.21	
	165	0.06	0.27	0.23	0.28	
	163	0.18	0.27	0.29	0.30	
242	241, 244	0.10	0.09			E - W 48 ft
251	252	0.01	0.04			E - W 20 ft East side

* Stope 164 mined in two stages, assumed predicted displacement equally divided between stages.

** Measured by borehole extensometer.

*** Predicted by finite-element analysis.

all stages of mining with the 163 pillar slash being a notable exception.

Although there is overall agreement between measured and predicted movements over the 45 ft in the north-south direction the individual increase for each block in some cases do not correspond. The measured movements show that adjacent stopes 162 and 164 and the 163 pillar slash produced the major movement, whereas the predicted movements show that the mining of pillars 161 and 165 should also have produced significant movements. The possible causes which could produce these discrepancies are discussed at the end of this section.

The deformation measured in pillar 242 resulting from the mining of blocks 241 and 244 is in close agreement with the predicted movement. The comparison for pillar 251 is not as good although the order of magnitude is the same. Movements measured in pillar 228 (Figure 4) are not included in Table 1 since

most movement was concentrated at a weakness plane and is not predicted by this finite-element analysis.

The comparison between measured pillar stresses and those determined by the model are shown in Table 3. For the assumed field stress ($S_o = 2,500$ psi, $S_t = 5,000$ psi), it can be seen that the measured stresses are roughly half the predicted stresses. The fact that there is three-dimensional transfer of stresses around the actual pillars undoubtedly is a major reason for these differences.

In spite of this probable explanation, further analyses were made varying the field stress. These cases might be considered as producing two-dimensional conditions equivalent to the actual three-dimensional transfer; in other words, only a fraction of the field stress is being transferred into the pillar, the other part being diverted above and below the stopes. It can be seen that if field stresses of $S_o = 1,600$ psi and $S_t = 4,000$ psi are used, the agreement with the measured stresses is very good. In an alternate

TABLE 3
Stresses in Pillars at the MacLeod Mine,
Measured vs Predicted

Pillar Site	Model Excavations to Approximate Actual Conditions	Pillar Stresses		Remarks
		Measured psi	Predicted psi	
242	1, 3, 5, 6, 7	2600	6000	Pillar breadth 66 ft compared to 80 ft for model. Length of stopes 200 ft which is less than about 600 ft required to fulfill the conditions for a two-dimensional analysis.
251	1, 3, 5, 6, 7	3000	6000	Pillar breadth 60 ft
163	1, 3, 5, 6, 7	3700* 3000 1400*	6000 3300 580	Calculated from Figure 3 at 520 days. $S_o = 1,600$ psi, $S_t = 4,000$ psi. $S_o = 600$ psi, $S_t = 7,000$ psi. Note that model is not a good representation of actual conditions as there should be an additional block excavated adjacent to No. 5 representing pillar 165.

* $\delta = (\Delta \sigma_p - \mu (\Delta \sigma_t + \Delta \sigma_z)) H/E$; $\Delta \sigma_t = -S_t$; $\Delta \sigma_z = 0$; $H = 106$ feet.

case of $S_o = 600$ psi and $S_t = 7,000$ psi the agreement is not good. The seeming paradox of the measured pillar stresses, recorded in Table 3, varying with the field stresses is explained by the fact that deformation is actually measured from which pillar stresses are calculated using assumed values of the field stresses.

In summary, the finite-element analysis on the two-dimensional model predicts movements and stresses greater than those measured in situ. Also it predicts that mining of blocks beyond the immediate stopes on either side of the pillar have a much greater effect on the longitudinal north-south stresses and deformations than is observed in practice. Probably the main reason for these discrepancies is that part of the field stress is being diffracted above and below the stopes instead of all on the pillars as in the model. This diffraction in the third dimension would result in a reduction in the pillar stresses and deformations. In addition, blocks more than one stope distance away from the pillar are nearer to the solid ground above and below the stopes, and the stress field is more likely to be transferred over this shorter distance rather than over the longer distance to the pillar. This would explain why mining beyond the immediately adjacent stopes produces very little deformation in the north-south direction. Other factors which could explain the discrepancies are that the assumed field stresses of $S_o = 2,500$ psi and $S_t = 5,000$ psi are too large and should not only

be reduced but also the S_o/S_t ratio increased to explain the small measured movements near the hanging wall and footwall. Also, a larger deformation modulus than the value of 10×10^6 psi, while not significantly altering the stresses, would reduce the predicted deformations.

In conclusion, it would seem that the three-dimensional aspects of the actual situation makes it difficult to predict accurately using a two-dimensional model. However, by using this model the mechanics of stress transfer and the behaviour of the structure can be more readily understood. At the same time, it is conceivable that the actual field stresses could be modified by a reduction factor based on some kind of simple three-dimensional analysis the purpose of which would be to determine the equivalent conditions for a central section to be analyzed in two dimensions.

Case History of Pillar Cracking

Noticeable cracking has occurred in several of the pillars mined since underground operations commenced in 1949. At depths from 800 to 1,500 ft, pillar cracking has caused sloughing of the pillar walls and in some cases offset blast holes. Pillar cracking is considered the first sign of instability, and while the whole pillar is not in a state of failure the tensile and shear strengths on certain planes of weakness have been overcome.

Two areas in the west section of the mine (Figure 1), one almost directly above the other, are examined.

Figure 8 shows the locations of observed cracks on the H2, M1-3 and M1-2 levels in Area 1. This area was about 500 feet along strike with the pillars 225 to 300 ft long down-dip. Mining proceeded over a period of 22 months with pillar cracking, and sloughing developing in the final 11 months. The cracks were of three main types: those parallel and near to the sides of the pillar, which are occasionally 1/2 in. wide; those striking in a northwesterly direction; and those striking in a northeasterly direction.

After the mining of 127 stope, partial mining of 125 and 123 stopes and removal of the 130 pillar, cracking was observed in pillar 128. Extensive sloughing took place from the sides of the 124 and 126 pillars, which were probably caused by cracks parallel to the sides of the pillars. Sloughing was also reported from the back of the 125 stope and was thought to be associated with a 15-ft intrusive cutting across the stope.

Figure 9 shows the locations of the observed cracks on the M1, M2-2 and M2-1 levels in Area 2. This area was about 1,000 ft along strike with the pillars 390 ft long down-dip. A thrust zone separated Areas 1 and 2. The direction of the cracks is similar to that observed in Area 1.

Stopes 231, 233, 235, 237 and the block 223 to 225 were mined over a period of 54 months before any pillar blasts. No cracks were observed during this time. Pillar 232 was blasted first, followed by a main portion of pillar 234. Following these blasts a buttress left on the hanging wall at pillar 234 cracked and sloughed off at the M2-1 sub-level. Pillar 236 was the next pillar blasted which produced a 500-ft-long opening to the east of pillar 230.

The hanging wall section of stope 229 was then mined, which produced extensive cracking and sloughing of pillar 230. Cracks up to 1 1/2 in. wide developed in the centre crosscuts on the first and second sub-levels and numerous cracks were observed in the hanging wall and footwall drifts.

The 230 pillar blast produced prominent cracks in the 228 crown pillar on the M1 level. During the mining of stope 227, additional cracks were observed in pillars 226 and 228,

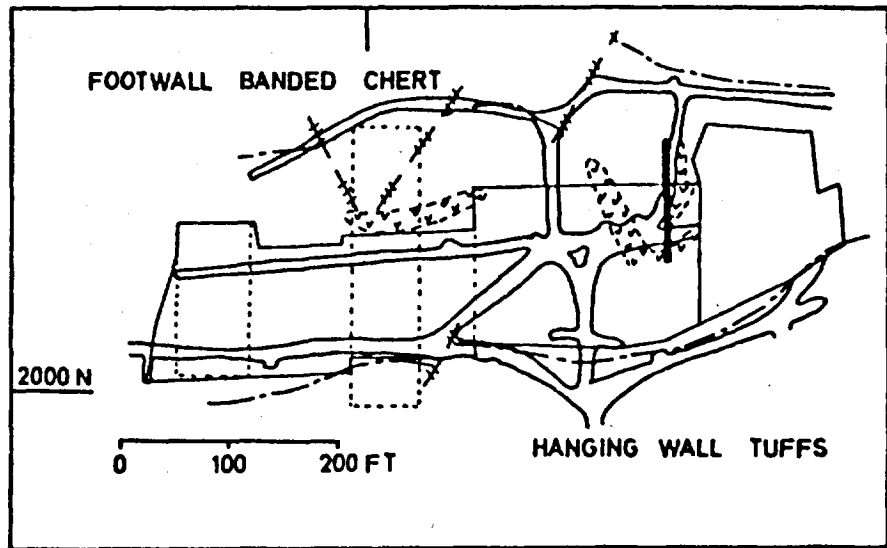
with the extensometer monitoring the movement of the cracks in pillar 228 as shown in Figure 4. These two pillars were the last to be blasted above the M2 level in the west section of the mine.

The 41 cracks observed in Areas 1 and 2 can be categorized into three main groups as shown in Table 4. The cracks parallel to the sides of the pillars, set No. 1, mainly occur within 15 ft of the pillar side. These cracks are probably extension fractures and are directly related to the lateral expansion of the pillar, and in some cases result in pillar sloughing. The diagonal cracks, sets No. 2 and 3, probably result from shear movement, which occurs when the frictional resistance is overcome along the joint and fault planes. These crack sets are mainly concentrated in the central portion of the pillar and rarely penetrate into the hanging-wall or footwall.

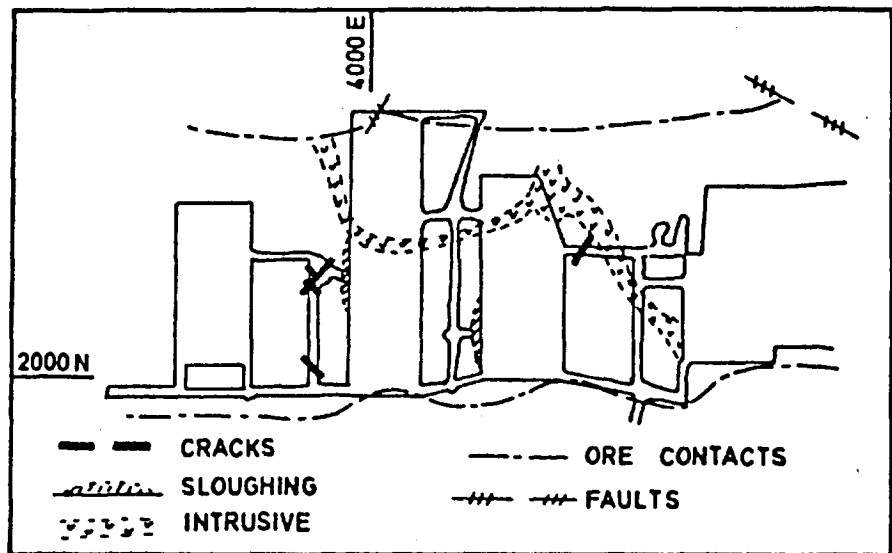
The progressive pillar deterioration can be visualized as the result of two processes: relief of stresses at the pillar sides permits extension fractures in the rock, not necessarily along any structural weakness planes; shear stresses produce sliding between blocks of rocks, the magnitude, location and initiation of movement is dependent on the structural weakness planes. Considering the susceptibility of the diagonal fault and joint planes to shear movement, it can be deduced that:

1. those planes which intersect both sides of the pillar have the least resistance;
2. those which intersect one side and either the hanging wall or footwall require crushing of the rock or intersecting planes of weakness for movement to occur; and
3. those planes which intersect both the hanging wall and footwall have the greatest resistance. It follows that wide pillars are more stable than narrow pillars since only planes, almost at right angles to the direction of stress, can intersect both sides of the pillar.

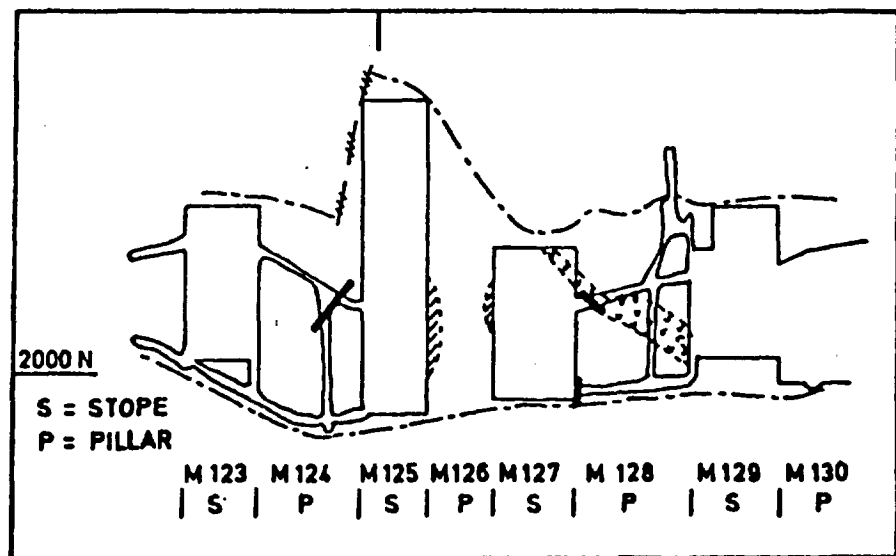
The relative magnitude of the stresses acting parallel and normal to the fault planes will determine whether movement occurs. Using the finite-element method of analysis the stresses parallel and normal to the north 30° west and north 30° east fault and joint systems, were calculated. Field stresses of 1,600 psi (S_0) perpendicular to the hanging wall and footwall and 4,000 psi (S_1) parallel to strike were used. An opening of 340 ft was taken on one side of an 80-ft-wide pillar and a 60-ft opening on the



PLAN OF H-2 LEVEL

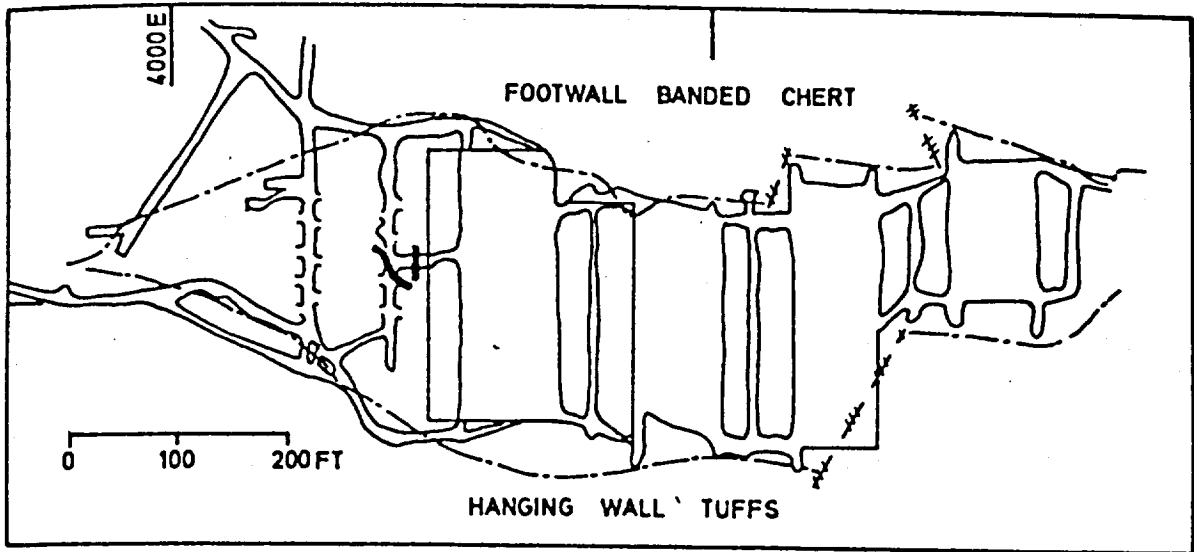


PLAN OF M1-3 SUB-LEVEL

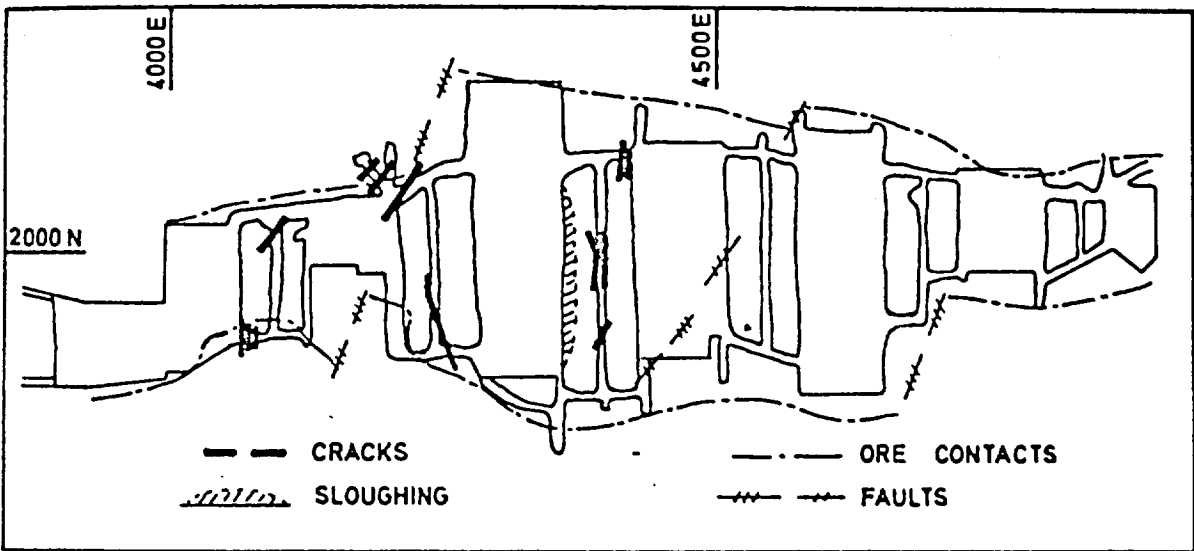


PLAN OF M1-2 SUB-LEVEL

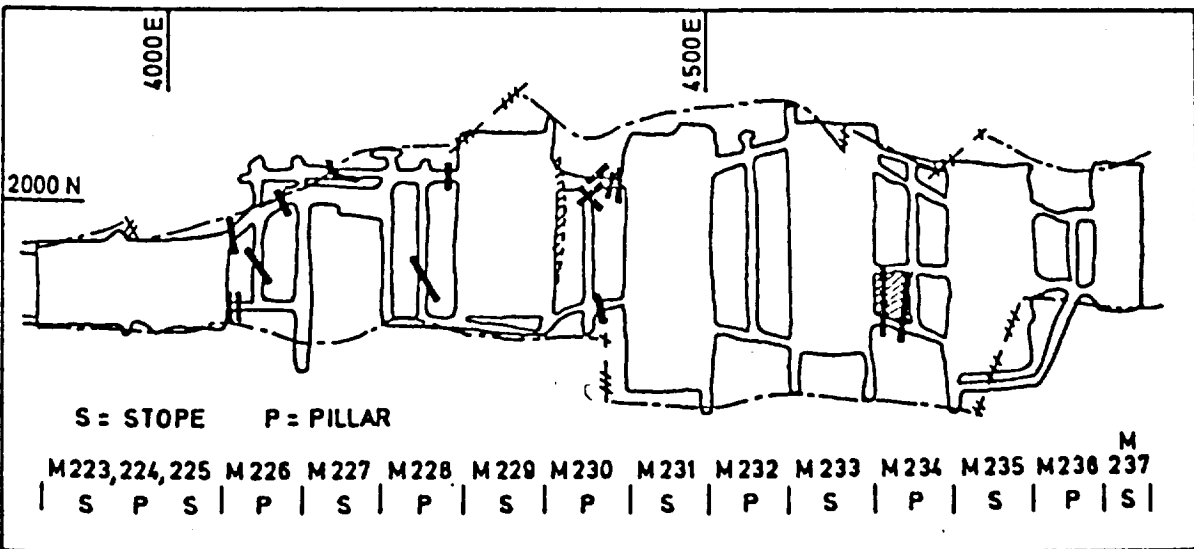
FIGURE 8 – Location of pillar cracks in area 1



PLAN OF M1 LEVEL



PLAN OF M2-2 SUB-LEVEL



PLAN OF M2-1 SUB-LEVEL

FIGURE 9 - Location of pillar cracks in area 2

TABLE 4
Details of Crack Survey

Set No.	Direction of Cracks	No. of Cracks	Remarks
1	north $\pm 10^\circ$	20	Parallel to pillar sides, not associated with any prominent joint or fault system;
2	north 30° west $\pm 15^\circ$	12	Associated with a steeply dipping fault system;
3	north 30° east $\pm 10^\circ$	9	Associated with a vertical joint system.

other side. The stresses at different locations along the pillar centre line between hanging wall and footwall are given in Table 5.

A high, parallel to normal, stress ratio (τ/σ) indicates the greatest likelihood of shear movement along the planes. The calculated results confirm that the central area of a pillar is more susceptible to shear movement than that near the hanging wall or footwall.

The propagation of pillar cracks has been observed in several pillars and monitored by extensometers in two pillars. The measurements indicate that even during the first stages of mining around a pillar, movement occurs on the fault and joint planes and only during the last stages of mining are the cracks readily visible. The worst cases of pillar cracking occur where an opening at least 300 ft long exists on one side of a pillar and the stope on the other side of the pillar is being mined, e.g. pillar 230 as stope 229 was mined and pillar 228 as stope 227 was mined.

These observations on pillar cracking are only relevant to the west section of the mine. A preliminary structural-geological study in the east section indicates that the fault and joint sets are parallel to the pillar sides. In this case, lateral expansion and the associated cracks should be more prominent than the shear movement along the diagonal faults and joints experienced in the west section.

Conclusions

The research program provided:

1. information on the usefulness of various types of instrumentation;
2. an understanding of the pillar stresses and deformations associated with this method of mining;
3. data for the development of an analytical approach for predicting stresses and deformations; and
4. an understanding of the factors involved in pillar stability.

Extensometers were found to give the most useful information on:

1. the stability of the pillars
2. the location and movement at planes of weakness
3. the extent of load transfer to a pillar, and
4. an estimate of the increase in pillar stress due to mining. Stress measurements, with the equipment used, can give order of magnitude values and define the directions of the principal stresses. Sonic measurements can be used to estimate the elastic modulus and Poisson's ratio of the rock mass. At this mine, this method was not suitable for determining zones of fracture since cracking was already visible before any significant change in sonic velocity occurred. Microseismic measurements indicate working of the rock, but it is difficult to define the origin and significance of the noises. It is considered

TABLE 5
Calculated Stresses Acting on Joint and Fault Planes

Location	Both North 30° West and North 30° East Planes		
	Parallel Stress (τ)	Normal Stress (σ)	τ/σ
Hanging wall or Footwall	600 psi	3,000 psi	0.2
2/3 Distance from Centre	900 psi	1,800 psi	0.5
1/3 Distance from Centre	1,450 psi	1,200 psi	1.2
Centre	1,700 psi	950 psi	1.8

that extensometer measurements provide the same information and are more easily interpreted.

Extensometer measurements in pillar 163 indirectly confirm the field stress measurements as to the direction of the principal stresses, parallel to strike being the major, perpendicular the intermediate, and vertical the minor. Measurements in pillar 163 also indicated that load is transferred to the pillar while the immediately adjacent stopes are being mined. In this location, mining greater than one stope distance from the pillar means that solid ground is nearer above and below the stopes and the load will naturally be transferred over the shorter span. However, this will not always be the case on the second and third levels and it is expected that pillars will be affected by mining over a greater distance as the spans increase.

The finite element analytical model gave values of pillar deformation and stress of the same order of magnitude at those measured. However, there were a number of discrepancies due to trying to represent a three-dimensional stress and geometrical condition as a two-dimensional problem. The possibility exists of modifying the actual field stresses to give equivalent conditions in two dimensions. This type of analysis may be useful in determining the shear and normal stresses acting on the planes of weakness and in conjunction with in situ measurements provide an estimate of pillar strength.

D.G.F. Hedley

Education — B. Sc., mining engineering, Royal School of Mines, 1963; Ph D, rock mechanics, University of Newcastle-upon-Tyne, 1965.

Employment Summary — 1965-67, National Research Council of Canada post-doctorate research fellowship. At present, research scientist, Mines Branch Elliot Lake Laboratory, Department of Energy, Mines and Resources, Elliot Lake, Ont.

G. Zahary

Education — B. Sc., mining engineering, University of Alberta, 1955; M Eng, rock mechanics, McGill University, 1963.

Employment Summary — 1958-61 and 1964-66, mining engineer at Steep Rock Iron Mines and International Minerals and Chemical Corp. (Canada). At present, research scientist, Mines Branch Elliot Lake Laboratory, Department of Energy, Mines and Resources, Elliot Lake, Ont;

The measurements taken at this mine together with the geological study and survey of pillar cracking indicate that the fault and joint planes of weakness, rather than the strength of the rock substance are the main factors determining pillar stability. The development of these cracks is most noticeable where there is a large opening on one side and mining is advancing in the adjacent stope. In addition the number of cracks observed in the pillars on the second level (Area 2, Figure 9) is greater than those observed on the first level (Area 1, Figure 8). Consequently, the frequency of cracking seems to increase with depth and may be indicative of increasing pillar stress with depth.

Acknowledgments

The authors would like to acknowledge the contribution made by each of the following: the management of the Algoma Ore Division for their participation in the research program; the geological staff at the MacLeod mine who took many of the measurements; Dr. G. Herget who worked on the structural geology aspects; F. Grant, Y. Yu, W. Zawadski, A.V. St. Louis and H. Montone of the Elliot Lake Laboratory; and S. Cook, J. Sullivan and W. Rowe of the Rock Mechanics Laboratory, Ottawa, who participated in the project.

Reference

Wilson, E.L. *Finite-Element Analysis of the Two-Dimensional Structures*, 1963. U. of Calif, Structures and Materials Res. Dept. of Civil Eng. No. 63-2.

H.W. Soderlund

Education — B.Sc., University of Saskatchewan, 1950.

Employment Summary — 1950-51, engineer at Magnet Consolidated Gold Mine and Lake Shore Gold Mine; 1951-68, geologist, planning engineer and mine superintendent at the Ore Division of the Algoma Steel Corporation, Limited; at present, chief engineer, Ore Division at Algoma.

D.F. Coates

Education — B. Eng, McGill University, 1948, M. Eng., McGill University, 1954; MA, Oxford University, 1954; Ph D, McGill University, 1965.

Employment Summary — 1951-59, lecturer and supervisor of graduate research at McGill and Carleton universities; 1959-63, consulting engineer; 1963 to the present, head, Mining Research Centre, Mines Branch, Department of Energy, Mines and Resources, Ottawa, Ont.